

1 **Variability of BVOC emissions from a Mediterranean mixed forest in southern**
2 **France with a focus on *Quercus pubescens***

3

4 A.-C. Genard-Zielinski^{1,2}, C. Boissard², C. Fernandez¹, C. Kalogridis², J. Lathière², V. Gros², N.
5 Bonnaire² and E. Ormeño¹.

6

7 ¹ IMBE, Aix Marseille Université – CNRS – IRD – Univ. Avignon 3 Place Victor Hugo, F-13331 Marseille
8 cedex 3, France

9 ² Laboratoire des Sciences du Climat et de l'Environnement (LSCE-IPSL), Unité Mixte CEA-CNRS-UVSQ
10 (Commissariat à l'Énergie Atomique, Centre National de la Recherche Scientifique, Université de
11 Versailles Saint-Quentin-en-Yvelines), F-91198 Gif-sur-Yvette, France.

12

13 Correspondence to: Christophe Boissard (christophe.boissard@lsce.ipsl.fr)

14

15

16

17

18 **Keywords:** Isoprene, BVOC, biogenic emissions, *Quercus pubescens*, *Acer Monspessulanum*,
19 canopy, branch enclosure, Mediterranean area, O₃HP

20 Abstract

21

22 We aimed at quantifying Biogenic Volatile Organic Compounds (BVOC) emissions in June
23 from three Mediterranean species located at the O₃HP site (Southern France): *Quercus*
24 *pubescens*, *Acer monspessulanum* and *C. coggygia* (for isoprene only). As *Q. pubescens* was
25 shown to be the main BVOC emitter with isoprene representing $\approx 99\%$ of the carbon emitted
26 as BVOC, we mainly focused on this species. *C. coggygia* was found to be a non-isoprene
27 emitter (no other BVOC were investigated).

28 To fully understand both, the canopy effect on *Q. pubescens* isoprene emission and the
29 inter-individual variability (tree to tree and within canopy), diurnal variations of isoprene
30 were investigated from nine branches (seven branches located to the top of canopy at ≈ 4 m
31 Above Ground Level (AGL), and two inside the canopy at ≈ 2 m AGL).

32 *Q. pubescens* daily mean isoprene emission rates (ER_d) fluctuated between 23 and 98 μgC
33 $\text{g}_{\text{DM}}^{-1} \text{h}^{-1}$. *Q. pubescens* daily mean net assimilation (*Pn*) ranged between 5.4 and 13.8, and
34 2.8 and 6.4 $\mu\text{molCO}_2 \text{ m}^{-2} \text{ s}^{-1}$ for sunlit and shaded branches respectively. Both ER_d and
35 isoprene emission factors (Is) assessed according to Guenther et al., (1993) algorithm, varied
36 by a factor of 4.3 among the sunlit branches. While sunlit branches ER_d was clearly higher
37 than for shaded branches, there was a non-significant variability on Is (59 to 77 $\mu\text{gC g}_{\text{DM}}^{-1} \text{h}^{-1}$).
38 Diurnal variations of isoprene emission rates (*ER*) for sunlit branches were also
39 investigated. *ER* were detected at dawn 2h after *Pn* became positive and, for most of them,
40 exponentially dependent on *Pn*. Diurnal variations of *ER* were not equally well described
41 along the day by temperature (*C_T*) and light (*C_L*) parameters according to G93 algorithm.
42 Temperature had more impact than PAR in the morning emission increase, and *ER* was no
43 more correlated to *C_L* \times *C_T* between solar noon (maximum *ER*) and mid-afternoon, possibly
44 due to thermal stress of the plant. A comparison between measured and calculated
45 emissions using two isoprene algorithms (G93 and MEGAN) highlighted the importance of
46 isoprene emission factor Is value used, and some weakness in assessing isoprene emissions
47 under Mediterranean environmental conditions (drought) with current isoprene models.

48 1 Introduction

49

50 Isoprene (2-methylbuta-1,3-diene) is the most abundant Biogenic Volatile Organic
51 Compound (BVOC) released into the atmosphere with a global annual flux estimation of 400-
52 660 TgC.yr⁻¹ (Guenther et al., 2006). Once in the atmosphere and due to the high quantity
53 emitted, isoprene strongly impacts the atmospheric chemistry. Indeed, this molecule is going
54 to react quickly with the main oxidant compound (OH), leading to the formation of oxidative
55 highly reactive products in the atmosphere (Atkinson, 2000; Ciccioli et al., 1999; Claeys et al.,
56 2004; Steiner and Goldstein, 2007).

57 At a smaller scale, isoprene plays a key role in the tropospheric chemistry since, alike other
58 VOC, it is an ozone precursor in presence of NO_x and light (Atkinson, 2000). NO_x being
59 mainly emitted by anthropogenic sources, isoprene emissions occurring close to mega-cities
60 surrounded by large ecosystem areas (such as Mediterranean) can significantly contribute to
61 high O₃ levels in summer (Curci et al., 2009).

62 Isoprene emissions are well recognized to be strongly driven by temperature and light
63 conditions. Indeed, without any other environmental constraints, these two parameters
64 drive the diurnal cycle of isoprene emission (Guenther et al., 1991). More precisely, light
65 affects the photosynthetic processes which, in turn, impact the quantity of isoprene
66 precursor (especially Glyceraldehyde 3-Phosphate) for isoprene synthesis, and temperature
67 increases isoprene synthase activity (Niinemets et al., 2010b). As a result, it was shown that
68 the branch location inside a canopy is an important source of isoprene emission variability,
69 with significant lower isoprene emissions from shaded branches inside the canopy compared
70 to sunlit branches at the top of the canopy (Harley et al., 1994; Monson and Fall, 1989).

71 However, other factors can explain isoprene emission variability. In particular, the capacity
72 to emit isoprene (or emission factor Is) is intrinsically bound to the plant species. Guenther
73 et al. (1994) proposed therefore to divide isoprene emitter species into four groups with
74 negligible (<0.1 μgC g_{DM}⁻¹ h⁻¹), low (14 ± 7 μgC g_{DM}⁻¹ h⁻¹), moderate (35 ± 17 μgC g_{DM}⁻¹ h⁻¹)
75 and high (> 70 ± 35 μgC g_{DM}⁻¹ h⁻¹) emitter species.

76 In Europe, *Quercus pubescens* Willd. is one of the most important isoprene emitter species,
77 and represents thus one of the most significant biogenic isoprene sources in the
78 Mediterranean region (Keenan et al., 2009). Previously reported Is values were observed to
79 vary for this species in the Mediterranean area over a large range. Kesselmeier et al. (1998)

80 and Owen et al. (1998) assessed a fairly similar Is of 50 and 66 $\mu\text{gC g}_{\text{DM}}^{-1} \text{h}^{-1}$ respectively at a
81 site near Montpellier (France), which was 50% lower than what Simon et al. (2005) found
82 250 km from this site. On the other hand, Steinbrecher et al. (2013) observed a remarkable
83 Is stability from seedlings of various oak species (including *Q. pubescens*) originating from
84 different environmental climates (precipitation, temperature) and coming from different
85 European sites. Simpson et al. (1999) proposed in his European BVOC inventory review an Is
86 value of 53 $\mu\text{gC g}_{\text{DM}}^{-1} \text{h}^{-1}$ for *Q. pubescens*.

87 This emission factor variability represents one of the main uncertainties of BVOC emission
88 models. Parameters such as edaphic conditions, natural hybridization between plant species,
89 or environmental tree history have been suggested to impact the overall capacity of a plant
90 to emit isoprene.

91 This study was part of the CANOPÉE project which aimed at analysing and quantifying intra-
92 canopy processes in the reactive organic compound exchange between the biosphere and
93 the atmosphere, with a focus on isoprene (further details can be found at
94 <https://wiki.lsce.ipsl.fr/CANOPÉE>). An intensive field campaign took place at the Oak
95 Observatory at OHP (O₃HP), a Mediterranean site located in Southern France.

96 Our objectives during this campaign were, (i) to extensively screen, at the branch scale and
97 using dynamic enclosures, BVOC emissions from the O₃HP forest, with a focus on *Q.*
98 *pubescens* and, to a lesser extent, *Acer monspessulanum* L. whose emission data has never
99 been reported so far; *Cotinus coggygria* was also investigated in terms of isoprene alone; (ii)
100 to survey the canopy variability (tree to tree and within the canopy) and (iii) the diurnal
101 variability of *Q. pubescens* isoprene emissions, and (iv) to test the ability of two commonly
102 used algorithms to assess, under Mediterranean environment constraints, the observed
103 diurnal variations of isoprene emission.

104

105 **2 Methods**

106

107 **2.1 Experimental site**

108

109 BVOC measurements took place at the O₃HP experimental site located in the research center
110 'Observatoire de Haute Provence', 60 km north of Marseille (5°42'44" E, 43°55'54" N), at an
111 elevation of 650 m above mean sea level. The O₃HP (955 m²), free from human disturbance

112 for 70 years, consists of a flat homogeneous forest mainly composed of *Q. pubescens* ($\approx 90\%$
113 of the biomass and $\approx 75\%$ of the trees). The remaining 10 % of the biomass is mainly
114 represented by *A. monspessulanum* trees. The mean *Q. pubescens* diameter at 1.3 m is 8.8
115 cm ($n=272$) and the stage of the whole canopy closure was assessed by a mean leaf area
116 index of 2.2. Dry leaf production was assessed for *Q. pubescens* to range between 1.4 and
117 1.6 t y^{-1} . The O₃HP site was created in 2009 in order to study the downy oak (*Q. pubescens*)
118 forest ecosystem at soil and tree scale, under both natural and accentuated water stress
119 conditions (a control and a rain exclusion plot respectively) induced by a rainfall exclusion
120 device (an automated monitored roof deployed during rain events) set up over a part of the
121 O₃HP canopy. A dense network of sensors in the soil, under and over the canopy,
122 continuously recorded the climatic and edaphic parameters (air and soil temperatures and
123 relative humidity, photosynthetically active radiation or PAR). A two level metallic scaffold
124 allows the canopy access at two heights (under the canopy at 0.8 m and at the top of the
125 canopy at 4 m). For further details see <https://o3hp.obs-hp.fr>.

126

127 **2.2 Sampling strategy**

128

129 The experiment took place from 29 May till 19 June 2012. A total of nine different *Q.*
130 *pubescens* and one *A. monspessulanum* were studied for isoprene emissions during the
131 campaign. *C. coggygria* was found to be a non-isoprene emitter (no other BVOC were
132 investigated).

133 At the beginning of the campaign, in order to screen the composition of BVOC emissions and
134 monitor diurnal variations over a 24 h period, a PTR-MS was connected to an enclosure
135 system (described below) set up on one *A. monspessulanum* and one *Q. pubescens* sunlit
136 branch (*Am*, 2 June and *Qp4*, 1 June respectively). *Am* and *Qp4* were located in a clearing
137 40 m north of the O₃HP scaffold (Fig. 1) close to where the PTR-MS system was set up during
138 the CANOPÉE campaign (see Kalogridis et al., (2014)).

139 To further investigate the variability of isoprene emission at the canopy scale two strategies
140 were undertaken.

141 On the one hand, tree-to-tree variability was evaluated by studying three healthy and sunlit
142 *Q. pubescens* branches within the control (*Qp1*, *Qp2*, *Qp3*) and the rain exclusion (*Qp5*, *Qp6*,
143 *Qp7*) plot. On the other hand, variability of isoprene emissions between shaded and sunlit

144 branches was assessed on *Qp1* and *Qp2*. In addition to a sunlit branch, a shaded branch was
145 also studied for those two trees, approximately 2 m above ground (*Qp1_{shade}* and *Qp2_{shade}*).
146 Isoprene samples were collected on adsorbent cartridges.

147 When cartridges were used, isoprene emissions were sampled approximately hourly from
148 sunrise to sunset. One of the enclosures was maintained on the *Qp1* branch during the
149 whole campaign (15 days) in order to follow continuous diurnal variations of isoprene
150 emission rates during the concomitant isoprene canopy flux measurements carried out by
151 Kalogridis et al. (2014). The second enclosure was used to alternatively investigate, over one
152 to two days, isoprene emissions from the other eight branches selected (sunlit and shaded).
153 Concomitant microclimate (PAR, temperature, relative humidity) and physiological
154 parameters (net photosynthesis *P_n*, and stomatal conductance to water *G_w*) were
155 continuously monitored during the BVOC sampling.

156 No other *A. monspessulanum* branches were studied since the on-line PTR-MS screening
157 revealed very low BVOC emissions.

158

159 **2.3 Branch scale sampling methods**

160

161 Dynamic branch enclosures were used for sampling BVOC. Branches (mature leaves \approx 3
162 month old) were enclosed in a \approx 60 L PTFE (PolyTetraFluoroEthylene) frame closed by a
163 sealed 50 μ m thick PTFE film to which ambient air was introduced at 11–14 L min⁻¹ using a
164 PTFE pump (KNF N840.1.2FT.18[®], Germany). A PTFE propeller ensured a rapid mixing of the
165 chamber air and a slight positive pressure within the enclosure enabled it to be held away
166 from the leaves to minimise damage to the biomass. Microclimate (PAR, temperature,
167 relative humidity) inside the chamber was continuously (every minute) monitored by a data
168 logger (Licor 1400[®]; Lincoln, NE, USA) coupled to a RHT probe (relative humidity and
169 temperature, Licor 1400-04[®], Lincoln, NE, USA) and a quantum sensor (Licor, PAR-SA 190[®],
170 Lincoln, NE, USA); the later sensor was set up and maintained horizontally in the enclosure
171 and located close to the leaves. CO₂/H₂O exchanges from the enclosed branches were also
172 continuously measured using infrared gas analysers (IRGA 840A[®], Licor).

173 *P_n* (μ mol_{CO₂} m⁻² s⁻¹) was calculated using equations described by Von Caemmerer and
174 Farquhar, (1981) as follows:

175
$$Pn = \frac{F \times (Cr - Cs)}{S} - Cs \times E \quad \text{Eq. (1)}$$

176 where F is the incoming air flow rate ($\text{mol}_{\text{H}_2\text{O}} \text{s}^{-1}$), Cs and Cr are the sample and reference CO_2
 177 molar fractions respectively ($\mu\text{mol}_{\text{CO}_2} \text{mol}^{-1}$ or ppm), S is the leaf area (m^2), $Cs \times E$ is the
 178 fraction of CO_2 diluted in the water evapotranspired ($\mu\text{mol}_{\text{CO}_2} \text{m}^{-2} \text{s}^{-1}$), and E is the
 179 transpiration rate ($\text{mol}_{\text{H}_2\text{O}} \text{m}^{-2} \text{s}^{-1}$) calculated as follows:

180
$$E = \frac{F \times (Ws - Wr)}{S \times (1 - Ws)} \quad \text{Eq. (2)}$$

181 where Ws and Wr are the sample and reference H_2O molar fractions respectively ($\text{mol}_{\text{H}_2\text{O}}$
 182 mol^{-1}).

183 Gw ($\text{mol}_{\text{H}_2\text{O}} \text{m}^{-2} \text{s}^{-1}$) was calculated using the following equation:

184
$$Gw = \frac{E \times \left(1 - \frac{Wl + Ws}{2}\right)}{Wl - Ws} \quad \text{Eq. (3)}$$

185 where E and Ws are described in equation (2), Wl is the molar concentration of water
 186 vapour within the leaf ($\text{mol}_{\text{H}_2\text{O}} \text{mol}^{-1}$) calculated using the equation :

187
$$Wl = \frac{VP_{sat}}{P} \quad \text{Eq. (4)}$$

188 where VP_{sat} is the saturated vapour pressure (kPa), and P is the atmospheric pressure (kPa).

189 Air flow rates were controlled by mass flow controllers (Bronkhorst) and all tubing lines were
 190 PTFE-made.

191 Total dry biomass matter (DM) was assessed during this study for each sampled branch by
 192 manually scanning every leaf enclosed in the chamber and applying an area factor (AF)
 193 conversion extrapolated from concomitant measurements made on the same site. For top
 194 and shaded canopy branches, mean (range) DM measured during this study was 0.16 (0.01 -
 195 0.45) and 0.10 (0.01 - 0.38) g_{DM} respectively, and mean (range) AF was 13.17 (0.82 - 36.67)
 196 and 11.98 (2.10 - 41.85) cm^{-2} respectively. A mean leaf to mass area ratio (LMA) of $123.2 \pm$
 197 1.0 ($n=5$ trees) and 87.1 ± 1.8 $\text{g}_{\text{DM}} \text{m}^{-2}$ ($n=15$ trees) was then assessed for sunlit and shaded
 198 branches respectively. Since the sampled *A. monspessulanum* was not located into the
 199 protected O_3HP site, DM was assessed directly by cutting off the branch, drying and
 200 weighting foliar biomass; LMA was $75.4 \text{ g}_{\text{DM}} \text{m}^{-2}$.

201 Branch enclosures were mostly installed on the previous day before the first emission rate
 202 measurement took place, and, at least, 2 h before.

203 For BVOC screening, the PTR-MS was connected to the enclosure system with a 25 m length
 204 $\frac{1}{4}$ " PTFE tubing (not heated) in order to follow, on-line, the rapid diurnal variations of BVOC

205 emission rates from a *Q. pubescens* and an *A. monspessulanum* branch; flow rate entering
206 the chamber was fixed at 14.7 L min⁻¹ (for details on PTR-MS system see Kalogridis et al.,
207 2014).

208 Due to the number of samples collected during this study, BVOC sampled on cartridges were
209 analysed by the two partnered laboratories (IMBE, LSCE) using very similar analytical
210 techniques. BVOC concentrations were measured in both the inflowing and the outflowing
211 air by passing at 0.1 L min⁻¹ for 1-3 min through adsorbent cartridges: Chrompack glass tubes
212 6.1 od, 150 mm length packed with 0.06 g Tenax TA and 0.14 g Carbotrap B, and Perkin
213 Elmer stainless-steel (SS) tubes 6.1 mm od, 90 mm length packed with 0.3 g Tenax TA for
214 IMBE and LSCE respectively. Sampling rates were controlled by mass flow controllers. Before
215 measurement, tubes were preconditioned at 300 °C for 2-3 h under continuous helium
216 purge. During sampling, glass tubes were protected from direct sunlight with an aluminium
217 foil. Tubes were removed from a cold box located close to the enclosures just before the
218 measurements. Subsequent to sampling, tubes were sealed with Swagelock end caps and
219 PTFE ferrules and stored at 4 °C before laboratory analyse within the following three weeks.
220 Ozone was removed from sampled air by placing PTFE filters impregnated with sodium
221 thiosulfate (Na₂S₂O₃) onto the sampling lines accordingly to Pollmann et al. (2005).

222 BVOC emission rates (*ER*) using PTR-MS and cartridges were calculated by considering the
223 BVOC concentrations in the inflowing and outflowing air as:

$$224 \quad ER = Q_0 \times (C_{out} - C_{in}) \times B^{-1} \quad \text{Eq. (5)}$$

225 where *ER* is expressed in µgC g_{DM}⁻¹ h⁻¹, *Q*₀ is the flow rate of the air introduced into the
226 chamber (L h⁻¹), *C*_{out} and *C*_{in} are the concentrations in the inflowing and outflowing air (µgC L⁻¹)
227 and *B* is the total dry biomass matter (g_{DM}).

228 Intercomparison exercises between isoprene determination using both, IMBE and LSCE
229 cartridges, and the on-line PTR-MS, showed a mean difference (bias) between 4.0 and 8.6 %.

230 In addition to these parameters recorded inside the enclosures, daily mean PAR,
231 temperature and relative humidity were recorded above the canopy (6 m) during the
232 campaign and are presented in Figure 2a together with the mean daily soil water content
233 (Sw, Fig. 2b) obtained in the control and the rain exclusion plots (mean of 6 and 5 different
234 probes respectively).

235

236 2.4 Analytical methods

237

238 BVOCs collected into glass and SS cartridges were analysed using similar GC-MS techniques.

239 Glass tubes were analysed with a gas chromatograph (GC, HP 6890N[®]) coupled to a thermal

240 desorption injector (Gerstel TDS3/CIS4[®]) and a quadrupole mass selective detector (MSD,

241 HP 5973[®]). Sampling tubes were thermally desorbed at 250 °C with carrier gas (He) flowing

242 at 50 mL min⁻¹ for 10 min. Isoprene was re-concentrated onto a Carbotrap B cold trap

243 maintained at -50 °C. Secondary desorption was set up at 250 °C for 3 min. An “Al/KCl”

244 capillary type column (30 m × 0.250 mm i.d., 5 µm thickness film) was used for the analysis

245 using helium (5.6, Linde gas) as carrier gas at 1 mL min⁻¹ and the following temperature

246 program: 40 °C (1 min) to 200 °C (1 min) at 20 °C min⁻¹. The MS detector was set up at 250 °C

247 in scan mode with m/z ranging from 40 to 150 amu. The isoprene detection limit was

248 0.015 ng on column, corresponding to 3 pptv in air for a 1 L sample, with a level of analytical

249 precision better than 5 %. Under sampling conditions (similar flow rate, volume, biomass) 3

250 pptv corresponds to a minimum emission rate of 0.003 µgC.g_{DM}⁻¹ h⁻¹. Isoprene quantification

251 was achieved using a 5.00 ± 0.25 ppm diluted in N₂ certified gas standard (Air Liquide).

252 Desorption and quantitative analysis of BVOC from SS sampling tubes was carried out using a

253 Perkin Elmer ATD-300 automatic thermal desorption unit connected via a transfer line

254 heated at 220 °C to a Varian CP 3800 GC connected to a MSD, Varian Saturn 2200 MSD.

255 Compound desorption started at 225 °C for 10 min at 30 mL min⁻¹ onto a mixed Carbotrap B

256 and Carbosieve SII cold trap maintained at 0 °C. Secondary desorption was at 300 °C for

257 1 min. Compound separation was achieved using a fused silica capillary (25 m × 0.25 mm i.d.

258 coated with PoraBOND Q) porous layer open tubular column (PLOT). Initial oven column was

259 50 °C maintained for 3 min and then increased at 5 °C min⁻¹ up to 250 °C maintained for 10

260 min. The carrier gas was helium N6 at 1.2 mL min⁻¹. Samples were analysed in total ion

261 current mode, with m/z ranging from 20 to 250. The detection limit was 0.006 ng and

262 0.10 ng on column for isoprene and monoterpene respectively, corresponding to 1.2 pptv

263 and 40 pptv respectively in air for a 1 L sample, with a level of analytical precision better

264 than 7.5 %. Under sampling conditions (similar flow rate, volume, biomass) this correspond

265 to a minimum isoprene (monoterpene) emission rates of 0.0025 µgC g_{DM}⁻¹ h¹. Isoprene

266 quantification was made using a 3.97 ± 0.08 ppb in N₂ certified gas standard (NPL,

267 Teddington Middlesex, UK) for lower concentrations and a 3.90 ± 0.29 ppm in N₂ certified

268 gas standard (Air Liquide) for higher concentrations. Monoterpene quantification was made
269 by comparison with liquid standard (Fluka) appropriately diluted in MeOH. GC-MS
270 quantification was made for the ion m/z 67 and 93 for isoprene and monoterpene
271 respectively. Daily whole range calibrations were carried out.

272 Laboratory intercomparison between IMBE and LSCE analytical GC-MS system was carried
273 out by loading IMBE and LSCE isoprene standards in both types of tubes (glass and SS) over a
274 12–1400 ngC range. A coefficient of determination R^2 of 0.953 ($n=14$) and 1.000 ($n=7$) for the
275 GC-MSD HP 5973 and the GC-MSD Saturn 2200 respectively was found, with an estimation
276 bias ranging from 3 to 10 %, close to the analytical precisions. Likewise, no significant
277 differences were found between isoprene *in-situ* samples (0 - 150 ngC) simultaneously
278 collected into glass and SS cartridges on either the inflowing or outflowing air of the
279 enclosures ($n = 20$; slope = 1.05; $R^2 = 0.90$). No breakthroughs were observed for isoprene,
280 neither on laboratory tests (up to 1400 ngC) nor on *in-situ* samples (up to 660 ngC) for both
281 cartridges. No intercomparison was carried out for monoterpene analysis.

282 The overall uncertainty associated with emission rate measurements (including sampling
283 and analytical uncertainties) for both sets of cartridges was between 15 and 20 %.

284 Details on VOC determination using the PTR-MS can be found in Kalogridis et al. (2014).
285 Twelve masses were followed for both the *Acer* and the *Quercus* branch. Measurements of
286 the inflowing and outflowing air were made alternatively every 15 min, allowing an *ER*
287 assessment every 30 min.

288

289 **2.5 Statistics**

290

291 All statistics were performed on STATGRAPHICS® centurion XV by Statpoint, Inc. To compare
292 the relationship between BVOC emitted by *A. monspessulanum* and *Q. pubescens* branches
293 studied with PTR-MS and the $C_L \times C_T$ factor, we performed a linear regression analyses. In
294 order to check the absence of water stress impact on isoprene emission, slopes of the
295 regression lines between *ER* and $C_L \times C_T$ in the control and rain excluded plots were
296 compared using an ANOVA. The same test was used to compare differences between sunlit
297 and shaded branch emissions by comparing slopes of the regression lines between *ER* and C_L
298 $\times C_T$ for this modality. Moreover differences in *Pn*, *Gw*, and *Sw* between control and rain
299 excluded trees were analysed using Mann & Whitney tests (W).

300

301 **3 Results and discussion**

302

303 **3.1 Experimental site conditions**

304

305 During the first half of the campaign, the weather was fairly unstable, with few showers or
306 longer rains, in particular on 12 June which was rainy most of the day, and an ambient
307 temperature decreasing down to a mean daily value of about 13 °C. From 13 June and until
308 the end of the measurements, the weather became more stable, sunnier, warmer and dryer;
309 the daily mean air temperature increased constantly up to nearly 24 °C at the end of the
310 campaign, the ambient relative humidity decreased down to 40 %, and Sw in both plots
311 decreased down to 0.11 and 0.15 $L_{H_2O} L_{soil}^{-1}$ for the rain exclusion and control plot
312 respectively. From 6 June, Sw in the rain exclusion plot was systematically lower than in the
313 control plot (Fig. 2b). Indeed, the annual cumulated precipitation in 2012 in the rain
314 exclusion plot (data not shown) became significantly different since the beginning of May
315 and was around 30 % lower compared to the control plot (comparison of means, Mann &
316 Whitney test, $W=508.0$, $P<0.05$).

317

318 **3.2 BVOC emission screening in the O₃HP forest**

319

320 **3.2.1 *Q. pubescens* BVOC emissions**

321

322 BVOC emissions from *Q. pubescens* (obtained by PTR-MS; *Qp4*, Table 1) were consistent with
323 previous literature results (Owen et al., 1998; Simon et al., 2005). Indeed, *Q. pubescens* was
324 found to be a strong isoprene emitter, with a daily mean value of isoprene emission rate
325 (ER_{iso}) of 98 $\mu\text{gC g}_{DM}^{-1} \text{h}^{-1}$ representing, on average, 98.8 % of the carbon emitted by the *Qp4*
326 branch. The remaining 1.2 % was found to represent a negligible quantity of the carbon
327 assimilated as CO_2 and was, in decreasing order, composed by methanol, total
328 monoterpenes, acetone (altogether ≈ 84 % of the non-isoprene BVOC), and methyl-vinyl-
329 ketone (MVK) + methacrolein (MACR), and acetaldehyde whose emissions were of the order
330 of 0.1 $\mu\text{gC g}_{DM}^{-1} \text{h}^{-1}$. Since isoprene, and total monoterpene emissions have been observed to
331 be light and temperature dependent in this study, *Q. pubescens* emission factors (EF) could

332 be assessed using the G93 algorithm (Guenther et al., 1993) and are presented in Table 1 for
333 *Qp4*.

334 Methanol is thought to be produced by destruction of wall cells during growth or during leaf
335 senescence (Galbally and Kirstine, 2002). It could be, both, a non-stored or stored compound
336 in the water compartments of the cell, such as vacuoles. However, since *Qp4* methanol
337 emissions were mainly exponentially dependent on temperature ($R^2 = 0.9$, $P < 0,001$) as
338 previously observed for *Picea* species (Hayward et al., 2004) and lemon trees (Fares et al.,
339 2011), it is likely that *Q. pubescens* methanol emission comes from an internal pool as
340 suggested by Seco et al. (2007). In the afternoon, methanol emissions became the main non-
341 isoprene compound emitted by *Q. pubescens*. Methanol release, as other alcohols, being
342 strongly stomatal dependent, its maximum relative contribution to the emitted carbon was
343 observed at dawn: up to 6.9 % of the carbon emitted as BVOC (data not shown) compared to
344 3.1 % and 0.8 % later in the morning and in the afternoon respectively. Although no
345 methanol emissions were previously reported for *Q. pubescens*, the mean emission rate
346 measured of $0.49 \mu\text{gC g}_{\text{DM}}^{-1} \text{h}^{-1}$ (or $130 \text{ ng g}_{\text{DM}}^{-1} \text{h}^{-1}$, or $1.13 \text{ nmol m}^{-2} \text{s}^{-1}$) is in the medium
347 range of the foliar emissions reviewed by Seco et al. (2007) for methanol emission from
348 emitters other than *Q. Pubescens*.

349 Total monoterpene emissions were more than 300 times lower than isoprene emissions, in
350 agreement with a factor of 250 found by Simon et al. (2005) for *Q. pubescens* studied under
351 Mediterranean conditions. Monoterpenes were found to be mainly under α -pinene and
352 limonene (67 % and 33 % respectively – data from cartridge samplings, not shown) and their
353 emission rates were more light and temperature dependent ('*de novo* emission') than only
354 temperature dependent ('pool emission') ($R^2 = 0.87$ and 0.64 respectively and $P < 0.001$).

355 As for methanol, no acetone emissions have been previously reported for *Q. pubescens*. The
356 mean emission rate of $0.20 \mu\text{gC g}_{\text{DM}}^{-1} \text{h}^{-1}$ (or $320 \text{ ng g}_{\text{DM}}^{-1} \text{h}^{-1}$, or $0.15 \text{ nmol m}^{-2} \text{s}^{-1}$) is also in
357 the medium range of the foliar emissions reviewed by Seco et al. (2007). The relative
358 contribution of acetone to the total BVOC emissions remained fairly stable along the whole
359 day of measurement (around 12.5 % of the non-isoprene BVOC), and was found to be
360 influenced by ambient light and temperature variations ($R^2 = 0.88$ and $P < 0.001$).

361 MVK+MACR are mainly secondary products of isoprene oxidation (Jardine et al., 2012). Our
362 study showed that MVK+MACR emission rates were highly ($R^2 = 0.97$, $P < 0.001$, $n = 28$)
363 correlated with ER_{iso} all along the diurnal cycle. A direct primary emission of these

364 compounds by the *Q. pubescens* branch could thus not be proved and values presented in
365 the Table 1 should be then considered as the upper limit for primary emissions from this
366 emitter.

367 Similarly, if acetaldehyde detected in our enclosure was mostly from primary biogenic
368 source (cell catabolism, see Fall et al., 1999 and Loreto et al., 2006), the emission rates thus
369 assessed ($0.09 \mu\text{gC g}_{\text{DM}}^{-1} \text{h}^{-1}$ or $165 \text{ ng g}_{\text{DM}}^{-1} \text{h}^{-1}$ or $0.10 \text{ nmol m}^{-2} \text{ s}^{-1}$) would be in the lower
370 range of the foliar emission rates reported in the literature for other plants (Seco et al.,
371 2007). As for methanol emissions, the relative contribution of acetaldehyde emissions to
372 total assimilated carbon was observed to peak in the morning (1.5 % in the morning
373 compare to 0.06 % in the afternoon).

374

375 **3.2.2 A. monspessulanum BVOC emissions**

376

377 *A. monspessulanum* total BVOC emissions ($< 1 \mu\text{gC g}_{\text{DM}}^{-1} \text{h}^{-1}$) were two orders of magnitude
378 smaller than the total *Q. pubescens* BVOC emissions ($> 100 \mu\text{gC g}_{\text{DM}}^{-1} \text{h}^{-1}$; Table 1). Isoprene
379 and methanol were the two dominant BVOC measured, with a daily mean emission rate of
380 0.33 and $0.23 \mu\text{gC g}_{\text{DM}}^{-1} \text{h}^{-1}$ respectively. Acetone, acetaldehyde, and total monoterpenes
381 were measured at lower rates, the latter being close to our detection limit. No foliar BVOC
382 emission values have been reported in the literature for *A. monspessulanum*. Nevertheless,
383 our findings confirm that, alike other *Acer* species (such as *Acer platanoides* L., *A. rubrum* L.,
384 or *A. saccharinum* L., Kesselmeier and Staudt, 1999), *A. monspessulanum* is a weak isoprene
385 or other BVOC emitter.

386 BVOC other than isoprene represented a lower fraction of the total carbon emitted in the
387 morning (≈ 33 %) than in the afternoon (≈ 66 %), methanol emission rates being, in the
388 morning, even higher than isoprene emission rates. Total BVOC emissions represented less
389 than 0.2 % of the assimilated carbon.

390 Ambient light and temperature variations influenced the diurnal emission variations of all
391 the measured BVOC except methanol which, as observed for *Q. pubescens*, was found to be
392 exponentially dependent.

393

394 To conclude, *Q. pubescens* appeared to be the main BVOC emitter in the O₃HP forest
395 compared to *A. monspessulanum*. Isoprene represented ≈ 99 % of the BVOC emitted by *Q.*

396 *pubescens*, with daily mean values as high as $\approx 100 \mu\text{gC g}_{\text{DM}}^{-1} \text{h}^{-1}$. Therefore, sections
397 hereafter focus on *Q. pubescens* isoprene emissions.

398

399

400

401 **3.3 *Q. pubescens* isoprene emission and associated gas exchange at the canopy scale** 402 **(tree-to-tree and within canopy)**

403

404 The additional drought imposed about one month before the beginning of the
405 measurements in the rain exclusion plot was not intense enough to significantly alter either
406 the capacity of *Q. pubescens* to assimilate CO_2 or to emit isoprene (comparison of regression
407 lines; $R^2 = 0.63$; $P > 0.05$). Although significant differences were observed on *Gw* with a value
408 for stressed trees half the one for control trees (Mann & Whitney; $P < 0.001$, Table 2),
409 isoprene emission has been suggested to not be constrained by stomatal conductivity as
410 pointed out by Niinemets and Reichstein, (2003). Thus water stress was not considered in
411 this study. As a result, trees growing in, both, the rain exclusion and the control plot were
412 pooled and analysed together without regard to their control/drought status.

413

414 **3.3.1 Plant physiology**

415

416 Daily *Pn* and *Gw* measured for top canopy branches varied between 5.4 and $13.8 \mu\text{molCO}_2$
417 $\text{m}^{-2} \text{s}^{-1}$ and 62.5 and $268.1 \text{mmolH}_2\text{O m}^{-2} \text{s}^{-1}$ respectively (Table 2). These values are in
418 agreement with observations previously reported by Damesin and Rambal, (1995) for *Q.*
419 *pubescens* in June (*Pn* of $10 \mu\text{mol m}^{-2} \text{s}^{-1}$ and *Gw* ranging from 50 to $150 \text{mmolH}_2\text{O m}^{-2} \text{s}^{-1}$).
420 *Gw* up to $450 \text{mmol H}_2\text{O m}^{-2} \text{s}^{-1}$ was reported for *Quercus ilex* L. in the Mediterranean
421 environment (Acherar and Rambal, 1992). Thus, despite the inherent modifications
422 occurring in the microclimate surrounding an enclosed branch (higher relative humidity -
423 especially during the night-time respiration - and warmer air temperature), no significant
424 impact on the physiology of the studied branches was observed. Similarly, the rain event of
425 12 June had no impact on *Pn* of *Qp1* or *Qp6* branches studied on this day. Shaded branches
426 *Qp1_{shade}* and *Qp2_{shade}* showed *Pn* values between 2.8 and $6.4 \mu\text{molCO}_2 \text{m}^{-2} \text{s}^{-1}$, more than half
427 the values on sunlit branches.

428

429 **3.3.2 Canopy variability of the branch isoprene emission rate**

430

431 As shown in Table 2, daily mean isoprene emission rates (ERd) from top of the canopy
432 branches were highly variable, fluctuating over one order of magnitude, between below 10
433 (*Qp1* and *Qp6*, 12 June) and up to 98 $\mu\text{gC g}_{\text{DM}}^{-1} \text{h}^{-1}$ (*Qp4*, 1 June). The lower ERd coincided
434 with reduced incident PAR and ambient temperature due to some rain events on 12 June.
435 Since *Qp4 Pn* was similar to *Pn* measured for the other trees (8.3 and between 5.4 and 13.8
436 $\mu\text{molCO}_2 \text{ m}^{-2} \text{ s}^{-1}$ respectively), the observed ERd range illustrates the importance of
437 environmental conditions on the amount of carbon *Q. pubescens* allocates to isoprene
438 emissions.

439 Daily mean ERd presented a high variability between sunlit branches (23 and 98 $\mu\text{gC g}_{\text{DM}}^{-1} \text{h}^{-1}$)
440 and shaded branches (4.0 and 13 $\mu\text{gC g}_{\text{DM}}^{-1} \text{h}^{-1}$). Daily mean *Qp1_{shade}* and *Qp2_{shade}* PAR were
441 reduced by a factor of six and ten respectively compared to PAR values recorded on *Qp1* and
442 *Qp2* sunlit branches. Consequently, shaded ERd (between 4.0 and 13 $\mu\text{gC g}_{\text{DM}}^{-1} \text{h}^{-1}$) were, on
443 average, between two and ten times lower than the values measured on the sunlit *Qp1* and
444 *Qp2* branches respectively; these values were the lowest ERd observed during the study. In
445 shaded branches, only 0.3 ± 0.2 to 0.5 ± 0.2 % of the assimilated carbon was emitted as
446 isoprene (C_{iso}), while C_{iso} for sunlit branches ranged between 0.4 ± 0.1 and 2.9 ± 1.0 %. Daily
447 mean C_{iso} was exceptionally high for *Qp4* (2.7 ± 2.2 %) and reached up to 6.5 % at solar noon.
448 Whatever their horizontal or vertical location in the canopy, for 2/3 of the sampled trees,
449 measured isoprene emission rates exponentially increased with *Pn*, except for *Qp3*, *Qp6* and
450 *Qp2_{shade}* (Fig. 3). As explained in the next section, *Qp3* was found to be dead in August,
451 although there were no visible sign when our study was conducted. *Qp6* was studied during
452 the only rainy day of our study (12 June, Table 2), and although its *Pn* was not affected, its
453 isoprene emissions were much lower than during sunny days. The range of ER_{iso} variation
454 observed for *Qp2_{shade}* being much lower than for other sunlit branches, it was difficult to
455 distinguish an exponential dependency to *Pn* as strong as for the other branches. Aside from
456 these particular cases, such an exponential relation between ER_{iso} and *Pn* implies that, even
457 when *Pn* reached the maxima values, the contribution of carbon fixed by each branch to
458 produce isoprene went on increasing.

459

460 3.4 Capturing *Q. pubescens* isoprene emission variability and providing estimates

461

462 3.4.1 Canopy variability of the isoprene emission factor I_s

463

464 Isoprene emissions being known to strongly depend on temperature and PAR variations, the
465 slope of measured isoprene emission rates vs the $C_L \times C_T$ product was calculated in order to
466 assess for each branch an emission factor I_s (Table 2) where C_L and C_T are light and
467 temperature dimensionless coefficients given by Guenther et al., (1993) from experimental
468 measurements (see supplementary section). For sunlit branches, I_s varied between 31 ± 8
469 and $138 \pm 10 \mu\text{gC g}_{\text{DM}}^{-1} \text{h}^{-1}$ for *Qp3* and *Qp4* respectively, which is in the range of values given
470 in the literature (50 , 66 and $118 \mu\text{gC g}_{\text{DM}}^{-1} \text{h}^{-1}$, Kesselmeier et al. (1998), Owen et al. (1998)
471 and Simon et al. (2005) respectively). A factor of more than two was found between, on the
472 one hand, *Qp4* emission factor and all the other branches in the control plot, and, on the
473 other hand, between I_s from *Qp1* and *Qp2* (72 ± 3 and $74 \pm 4 \mu\text{gC g}_{\text{DM}}^{-1} \text{h}^{-1}$ respectively) and
474 *Qp3* ($31 \pm 8 \mu\text{gC g}_{\text{DM}}^{-1} \text{h}^{-1}$). The overall factor of variability of 4.3 observed on I_s illustrate how
475 *in-situ* condition variations, even on a fairly homogenous site, can impact BVOC emissions.
476 Moreover, even under similar prevailing environmental conditions, the physiological status
477 variability that may exist between branches can lead to strong differences in the branch
478 capacity to emit isoprene. The smaller (by a factor of two) I_s observed for *Qp3* compared to
479 other O_3HP tree branches was *a posteriori* explained by the fact that this branch died in
480 August despite no injuries were visible during our study in June. By contrast Steinbrecher et
481 al. (2013) observed a remarkable stability on I_s values from seedlings of various oak species
482 originating from different environmental climates (precipitation, temperature) with a factor
483 of only 1.6 for *Q. pubescens* I_s .

484 Regarding the canopy shading effect, the studied shaded branches showed no significant
485 difference ($R^2 = 72.8$ and 89.2 for *Qp1* and *Qp2* branches respectively; $P > 0.05$) in their
486 capacity to emit isoprene (I_s of 77 ± 3 and $59 \pm 12 \mu\text{gC g}_{\text{DM}}^{-1} \text{h}^{-1}$ for *Qp1*_{shade} and *Qp2*_{shade}
487 respectively) compared to the sunlit branch of the corresponding tree, (I_s of 72 ± 3 and $74 \pm$
488 $4 \mu\text{gC g}_{\text{DM}}^{-1} \text{h}^{-1}$ for *Qp1* and *Qp2* respectively). This similarity occurred despite an observed
489 LMA vertical gradient: 87 ± 2 and $123 \pm 1 \text{ g m}^{-2}$ for shaded and sunlit branches respectively.
490 Such a gradient is similar to what Harley et al. (1994) reported for a *Quercus alba* forest: 75.4

491 ± 7.0 and $111.5 \pm 5.9 \text{ g m}^{-2}$ for shaded and sunlit branch respectively; when these authors
492 expressed I_s on a leaf area basis they observed significantly lower I_s values for a shaded
493 branch. Note that if the sunlit branch LMA value was used for assessing I_s from all our
494 branches (shaded and sunlit branches) - as it may be done in global upscaling inventory
495 when no appropriate LMA information is available - shaded I_s value would then become
496 significantly lower than I_s sunlit branches. As any other factors used when BVOC canopy
497 fluxes are extrapolated from branch to canopy scale, determination of appropriate LMA
498 should thus be as accurate as possible since it represents one of the biases of such an
499 exercise.

500 Based on our assessed I_s range (31 to $138 \mu\text{gC g}_{\text{DM}}^{-1} \text{ h}^{-1}$) and using an average branch scale I_s
501 value of $60 \mu\text{gC g}_{\text{DM}}^{-1} \text{ h}^{-1}$, Kalogridis et al. (2014) extrapolated a canopy isoprene emission
502 flux of $15 \text{ mg m}^{-2} \text{ h}^{-1}$, twice the mean canopy flux measured in June during this study by the
503 disjunct eddy covariance technique ($6.6 \text{ mg m}^{-2} \text{ h}^{-1}$). The authors pointed out that such a
504 factor of discrepancy is reasonable since it is in the range of uncertainties typically obtained
505 for upscaling exercises (see for example Guenther et al., 1995), and is within the range of the
506 tree to tree variability observed for *Q. pubescens* I_s on this site (a factor of 4.3). This
507 illustrates the limit of precision in BVOC canopy flux assessments, how much the I_s canopy
508 variability is extensively and intensively is studied.

509

510 **3.4.2 Diurnal variability: how well $C_L \times C_T$ captured the observed features?**

511

512 The diurnal range of isoprene ER variations observed over the seven sunlit different
513 branches studied (Fig. 4a) was found to fluctuate from day to day and with environmental
514 conditions (Fig. 4b). The maximum value observed on June 12 (rainy day) for the sun
515 exposed *Qp1* branch ($17 \mu\text{gC g}_{\text{DM}}^{-1} \text{ h}^{-1}$) was about five times lower than the maximum
516 observed at the end of the campaign (especially on 16 June, $78 \mu\text{gC g}_{\text{DM}}^{-1} \text{ h}^{-1}$) when weather
517 was much warmer and sunnier (Table 2 and Fig. 4b); it was about the same than the
518 maximum ER measured for the shaded branch *Qp1* at the beginning of the campaign (June
519 6-7, $\approx 20 \mu\text{gC g}_{\text{DM}}^{-1} \text{ h}^{-1}$). *Qp1* C_{iso} was the highest (up to 1.8 %, Table 2) at the end of the
520 campaign, compared to values < 1 % at the beginning of our measurements, which is
521 consistent with previous findings for *Q. pubescens* in June (0.62 to 1.8 %, Kesselmeier et al.,
522 1998).

523 Diurnal variations were studied in more detail during the *Qp4* high frequency measurements
524 carried out with the PTR-MS system. Positive P_n values were measured at 06:30, as soon as
525 PAR became detectable and increased at dawn in parallel of a C_L increase (Fig. 5). Detectable
526 isoprene emissions were observed only 2 h later (08:30), when ambient temperature
527 significantly increased (Fig. 5). Consequently, isoprene ER increased then as C_T . This finding
528 contrasts with previous studies (Owen et al., 1998) where *Q. pubescens* ER were more PAR
529 than temperature dependent. The morning delay observed between P_n and the isoprene
530 emission onset was found to correspond to a temperature increase dT of nearly 3 °C;
531 interestingly, a similar dT was observed for the *Qp1* branch when early morning
532 measurements were made. Temperature continued to significantly (compared to PAR)
533 impact isoprene until the maximum ER (229 $\mu\text{gC g}_{\text{DM}}^{-1} \text{h}^{-1}$ at 13:30). Between 13:30 and
534 17:30 isoprene emission remained constantly more temperature than light dependent. As
535 soon as PAR decreased (17:30), ER started to decrease to non-detectable values, while the
536 branch continued to assimilate CO_2 and P_n decreased only 1 h later. If the diurnal variations
537 of *Qp4* ER were mostly well described by $C_L \times C_T$ (in particular from dawn to midday
538 maximum and during the evening, the relative influence of light and temperature varied
539 along the day as presented in Figure 6: from 13:30 to 16:00 ER decreased from 220 to less
540 than 150 $\mu\text{gC g}_{\text{DM}}^{-1} \text{h}^{-1}$ at nearly constant $C_L \times C_T$; on the contrary, after 16:00, ER remained
541 close to 75 $\mu\text{gC g}_{\text{DM}}^{-1} \text{h}^{-1}$ although $C_L \times C_T$ fluctuated over nearly a factor of 3 (from 1.1 to 0.4).
542 Thus, after the solar noon, ER presented an overall reverse sigmoid shape diurnal
543 dependency with $C_L \times C_T$. The sudden decrease of ER at 13:30 while $C_L \times C_T$ remained
544 constant may illustrate a possible temperature midday stress of the branch, with an
545 emission falling down to a minimum value of $\approx 75 \mu\text{gC g}_{\text{DM}}^{-1} \text{h}^{-1}$. The thermal stress lasted
546 until 16:00 when isoprene emission regulation became again well correlated to $C_L \times C_T$.
547 Indeed, as reported by Niinemets et al. (2010a) heat stress could modify isoprene emission
548 by decreasing foliar metabolism. For instance, Funk et al. (2004) observed that during a heat
549 stress, an alternative source of carbon (carbon pool stored as carbohydrates) is used for
550 isoprene synthesis. As showed by Fortunati et al. (2008) for *Populus nigra* L., this alternative
551 carbon source being unaffected by temperature, our observations could illustrate a similar
552 uncoupling between isoprene emissions and $C_L \times C_T$ for *Q. pubescens*. Note that such a
553 response was also observed during water stress on *Quercus* species by Tani et al. (2011) who

554 suggested that, when photosynthesis was completely suppressed in the afternoon due to
555 severe water stress, the DMAPP content (or dimethylallyl pyrophosphate, the substrate for
556 isoprene synthase), was not high enough to maintain isoprene emission level as before
557 stress.

558

559 **3.4.3 Assessment of the diurnal profiles of *Q. pubescens* isoprene emission rates using** 560 **different algorithms**

561

562 Most of the different isoprene emission algorithms available for emission inventory are
563 based on the empirical leaf-level isoprene emission dependency on light and temperature
564 (Guenther et al., 1993). Among them, two were tested to evaluate their ability in assessing
565 the diurnal profiles of *Q. pubescens* isoprene emission observed in this Mediterranean
566 climate: (i) the simple and well known G93 algorithm (Guenther et al., 1993) which only
567 takes into account the instantaneous variations of incident light and ambient temperature –
568 hereafter referred to as G93, and (ii) the MEGAN parameterisation (Guenther et al., 2006), a
569 modified version of the former algorithm developed in an attempt to better capture the
570 emission seasonality through the consideration of the dimensionless γ_{age} factor dependent
571 on leaf age (here set at 0.6), the lower frequency variations (up to ten days) of
572 environmental conditions, and the impact of soil humidity through the γ_{SM} factor. The
573 algorithms were tested for *Qp4* branch using, both, an I_s value of $53 \mu\text{gC g}_{\text{DM}}^{-1} \text{h}^{-1}$ as
574 recommended by Simpson et al. (1999) for European *Q. pubescens* and our values obtained
575 in this study (72 and $138 \mu\text{gC g}_{\text{DM}}^{-1} \text{h}^{-1}$ for *Qp1* and *Qp4* respectively).

576 As a whole, both algorithms underestimated the *Qp4* measured ER (65 and 55 % for G93 and
577 MEGAN respectively, Fig. 7, Table 3) when Simpson et al. (1999) I_s value was used. This
578 discrepancy reached a factor of three for midday maximum emission (74 and $93 \mu\text{gC g}_{\text{DM}}^{-1} \text{h}^{-1}$
579 for G93 and MEGAN respectively compared to $229 \mu\text{gC g}_{\text{DM}}^{-1} \text{h}^{-1}$). When I_s values observed
580 during this study were employed, a much better agreement was found (a slight over- and
581 under- estimation of 16 and 8 %, and a root mean square error (RMSE) value \approx two and
582 three times lower for G93 and MEGAN respectively, Fig. 7, Table 3). The main bias was thus
583 found to be linked with I_s , since the general diurnal trend was roughly captured by both
584 algorithms ($R^2 > 0.91$ for all comparisons). However, note that the maximum *Qp4* emissions
585 calculated with both algorithms, were reached at 14:00 (MEGAN) and 15:30 (G93), later than

586 what was observed (13:30) and whatever the I_s value used. Besides, predicted ER remained
587 mostly constant until 16:00, while the observed emissions decreased to ER values 50%
588 smaller than the midday maximum as previously described and commented (section 3. 4.2).
589 Both algorithms being strongly dependant on temperature variations, such an observed
590 uncoupling between ER and elevated temperature (here higher than 33 °C) could not be
591 captured. ER evening decrease was predicted to occur more rapidly and earlier (18:00)
592 compared to *in-situ* observations, resulting in assessed ER of $\approx 10 \mu\text{gC g}_{\text{DM}}^{-1} \text{h}^{-1}$ compared to
593 the observed value of $75 \mu\text{gC g}_{\text{DM}}^{-1} \text{h}^{-1}$. On the contrary ER was assessed to occur much
594 earlier at dawn (6:30 compared to 8:00), thus as soon as P_n became positive, and was
595 overestimated by a factor of three by G93 over this period. Note that, for $Qp4$, the simpler
596 G93 algorithm performed almost as well as the more complex MEGAN parameterisation
597 (similar slope, R^2 and RMSE, Table 3).

598 Some similar findings were observed when G93 and MEGAN algorithms were tested over the
599 longer time series (13 days) of $Qp1$ diurnal measurements: when the measured I_s was
600 employed instead of the literature value, the underestimation of G93 and MEGAN was
601 reduced from 46 and 77 % respectively down to 27 and 68 % respectively, although RMSE
602 remained in the same range (Table 3). However, MEGAN performance became much weaker
603 ($R^2 = 0.15$) for $Qp1$, especially for the assessment of ER measured at the end of the 13 day
604 period (detailed data not shown), when much warmer and drier conditions settled down at
605 the O_3HP site. Indeed, the soil water content becoming lower than the wilting point used for
606 our soil type ($0.138 \text{ m}^3 \text{ m}^{-3}$ for clay soil type, Chen and Dudhia, 2001), the MEGAN γ_{SM} factor
607 was no longer 1 but significantly lowered most of the assessed isoprene emissions.
608 Unfortunately, the consideration of superficial (-0.1 m depth) soil moisture does not take
609 into account the tree ability to access to deeper water sources. Weather being cooler and
610 rainy at the beginning of the campaign, such a γ_{SM} modulation did not operate neither on
611 $Qp4$ measurements nor on the first day of the $Qp1$ measurements (γ_{SM} was 1). When γ_{SM} was
612 not considered anymore and set to 1 for all the $Qp1$ measurements, MEGAN performed
613 much better and assessed nearly 60 % of the observed variability compared to 15 %.
614 However, in this case, MEGAN only slightly reduced the overall $Qp1$ underestimation (≈ 60
615 %) compared to the simpler G93 algorithm (≈ 40 %), as for $Qp4$ tree.

616

617 4 Conclusions

618

619 The extensive study, at branch scale, of BVOC emissions from a Mediterranean forest
620 ecosystem dominated by *Q. pubescens* revealed that, unlike *Q. pubescens*, *C. coggygia* was
621 a non-isoprene emitter (no other BVOC were investigated) and *A. monspessulanum* was a
622 weak BVOC emitter (daily mean total $<1 \mu\text{gC g}_{\text{DM}}^{-1} \text{h}^{-1}$) with isoprene (36.3 %) and methanol
623 (25.3 %) being the two dominant emitted compounds (ERd, of 0.33 and $0.23 \mu\text{gC g}_{\text{DM}}^{-1} \text{h}^{-1}$
624 respectively); acetone, acetaldehyde and total monoterpenes were also measured at lower
625 rates.

626 *Q. pubescens* was found to be a strong isoprene emitter (≈ 99 % of the BVOC carbon mass)
627 with mean ER fluctuating between 23 and $98 \mu\text{gC g}_{\text{DM}}^{-1} \text{h}^{-1}$ for sunlit branches and 6.1 and
628 $11.5 \mu\text{gC g}_{\text{DM}}^{-1} \text{h}^{-1}$ for canopy shaded branches; methanol (ERd = $0.49 \mu\text{gC g}_{\text{DM}}^{-1} \text{h}^{-1}$; 0.5 % of
629 total BVOC) and total monoterpenes (ERd = $0.30 \mu\text{gC g}_{\text{DM}}^{-1} \text{h}^{-1}$; 0.3 % of total BVOC)
630 dominated the other emitted BVOC, but traces of acetaldehyde and acetone were also
631 measured.

632 For both shaded and sunlit *Q. pubescens* branches, most of the isoprene emission rates
633 exponentially increased with P_n , although P_n was half smaller for shaded than sunlit
634 branches. In shaded branches, a very small fraction of the recently assimilated CO_2 (C_{iso}) was
635 emitted as isoprene (0.25 - 0.5 %) whereas C_{iso} ranged between 0.5 - 1.8 % for sunlit
636 branches with a maximum of 6.7 % under elevated temperature and sunlight stress.

637

638 Tree to tree isoprene emission variability was high considering the sunlit branches ($n = 7$)
639 and, to a lesser extent, the shaded ($n = 2$) branches. ERd sunlit branches varied over a factor
640 of ten and emission factor I_s over a factor of 4.3 (between 31 ± 8 and $138 \pm 10 \mu\text{gC g}_{\text{DM}}^{-1} \text{h}^{-1}$).
641 Shaded branch variability was lower, a factor of three for ERd (between 4.0 and $13 \mu\text{gC g}_{\text{DM}}^{-1}$
642 h^{-1}) and not significant for I_s (between 59 ± 12 and $77 \pm 3.0 \mu\text{gC g}_{\text{DM}}^{-1} \text{h}^{-1}$).

643 Within the canopy (shaded vs sunlit branches), ERd varied by a factor of 25. However, this
644 difference between shaded and sunlit branches disappeared when I_s were calculated.

645 Such variability represents an assessment of the tree-to-tree and branch-to-branch
646 variability originating from *in-situ* conditions that should always be taken into account when
647 canopy BVOC fluxes are extrapolated from branch scale measurements. Thus, if experiments
648 conducted from saplings grown under near-natural, but controlled, conditions give a fairly

649 straightforward estimation of BVOC emissions by a plant, it cannot give the full picture
650 obtained by *in-situ* long term measurements.

651 The morning onset of isoprene emission rates was mainly driven by temperature and not *Pn*
652 which was, as expected, light triggered. By contrast, emission evening decline was mainly
653 correlated with PAR. In between, an uncoupling of isoprene emission with light and
654 temperature was noticed, with emissions starting to decline during the early afternoon
655 temperature stress whereas light and temperature remained stable.

656 If MEGAN and G93 algorithms succeed in capturing the overall diurnal pattern of isoprene
657 emission at the O₃HP, they significantly underestimated emissions by an average factor of up
658 to 3, and especially the midday maximum values when an *Is* other than those assessed for
659 this site was employed. Both algorithms were found to be very sensitive to *Is*, and showed
660 difficulties in properly assessing detailed isoprene diurnal variations, in particular at dawn
661 and when midday thermal stress occurred. Under water shortage, MEGAN performances
662 were even worse due to its inadequate local description of the soil moisture impact on *Q.*
663 *pubescens* isoprene emissions. When soil moisture was no more considered, MEGAN
664 performed similarly to the much simpler G93 algorithm for our June study; however, the G93
665 performance may be significantly reduced compared to MEGAN, when seasonal variations
666 are considered.

667 This comparison illustrates how uncertain global isoprene emission algorithms or models,
668 such as G93 and MEGAN, can be when employed for high temporal resolution air quality
669 predictions in Mediterranean areas.

670

671

672 **Acknowledgements**

673 We are very grateful to J.-P. Orts, I. Reiter, P. E. Blanc, J. C. Brunel and other OHP technical
674 staff for support before and during the campaign. We thank D. Coutancier, Post graduate
675 student of IUT d'Orsay for his efficient help in the analysis of LSCE sample tubes and the
676 result computing. We thank members of the DFME team from IMBE: S. Greff, C. Lecareux, S.
677 Dupouyet and A. Bousquet-Melou for their help during measurements and analysis. This
678 work was supported by the French National Agency for Research (ANR 2010 JCJC 603 01),
679 INSU (ChARMEx), CNRS National program EC2CO-BIOEFFECT (ICRAM project), CEA, and

680 Université Paris Diderot. We are grateful to FR3098 ECCOREV for the O₃HP facilities
681 (<https://o3hp.obs-hp.fr/index.php/fr/>), Europe (FEDER) and ADEME/PACA for Ph-D funding.

682 **List of Figures**

683

684 Fig. 1: Location of the studied *Q. pubescens* (*Qpi*) and *Acer monspessulanum* (*Am*) trees.
685 Branches *Qp4* and *Am* were located ≈ 40 m north of the O₃HP footbridge and BVOC emissions
686 were measured using an online PTR-MS. All other *Qpi* branches were sampled from the
687 O₃HP footbridge using adsorbent cartridges.

688 Black circles in the O₃HP area represent the assessed crown area of the sampled trees.

689

690 Fig. 2: Environmental conditions prevailing at the O₃HP site.

691 (a) Daily mean photosynthetically active radiation PAR ($\mu\text{mol m}^{-2} \text{s}^{-1}$), temperature T ($^{\circ}\text{C}$) and
692 ambient relative humidity RH (%) measured above canopy (6.5 m above ground), and, (b)
693 soil water content Sw ($L_{\text{H}_2\text{O}} L_{\text{soil}}^{-1}$) recorded in the control (C, 6 different probes) and rain
694 exclusion plots (S, 5 different probes) at -0.1 m.

695

696 Fig. 3: Isoprene emission rate ER_{iso} ($\mu\text{gC g}_{\text{DM}}^{-1} \text{h}^{-1}$) vs net photosynthetic assimilation P_n
697 ($\mu\text{mol}_{\text{CO}_2} \text{m}^{-2} \text{s}^{-1}$). Exponential dependency equation and determination coefficient R^2 are
698 given for each *Qpi* branch.

699

700 Fig. 4: (a) Diurnal variations of isoprene emission rate ER_{iso} ($\mu\text{gC g}_{\text{DM}}^{-1} \text{h}^{-1}$) measured from all *i*
701 *Qpi* branches sampled on the O₃HP footbridge, with (b) corresponding PAR ($\mu\text{mol m}^{-2} \text{s}^{-1}$) and
702 temperature T ($^{\circ}\text{C}$) conditions.

703

704 Fig. 5: Diurnal variations of *Qp4* isoprene emission rates ER_{iso} ($\mu\text{gC g}_{\text{DM}}^{-1} \text{h}^{-1}$) \pm SD vs the
705 corresponding net photosynthetic assimilation P_n ($\mu\text{mol}_{\text{CO}_2} \text{m}^{-2} \text{s}^{-1}$), PAR ($\mu\text{mol m}^{-2} \text{s}^{-1}$),
706 temperature T ($^{\circ}\text{C}$), and C_L and C_T parameters (as in Guenther et al., 1993).

707

708 Fig. 6: Diurnal variation of *Qp4* isoprene emission rate ER_{iso} ($\mu\text{gC g}_{\text{DM}}^{-1} \text{h}^{-1}$) vs $C_L \times C_T$ as in
709 Guenther et al., 1993 (1 June).

710 Plain purple diamonds are measurements between 08:00 and 14:00; plain orange diamonds
711 are measurements between 14:30 and 20:00. Polynomial best fit equation and
712 determination coefficient R^2 are given for morning (purple) and afternoon (orange).

713

714 Fig. 7: Comparison between *Qp4* isoprene emission rates ER_{iso} ($\mu\text{gC g}_{DM}^{-1} \text{h}^{-1} \pm \text{SD}$) measured
715 *in-situ* (1 June, purple diamonds) and assessed using isoprene emission algorithm as in (i)
716 Guenther et al. (1993) (G93, green diamonds) and as in (ii) MEGAN model (Guenther et al.,
717 2006, blue diamonds) using a leaf age factor γ_{age} of 0.6, a soil water factor γ_{SM} of 1 and a *Q.*
718 *pubescens* emission factor I_s value of ^(a) $53 \mu\text{gC g}_{DM}^{-1} \text{h}^{-1}$ (as in Simpson et al., 1999, open
719 diamonds), and ^(b) of $138 \mu\text{gC g}_{DM}^{-1} \text{h}^{-1}$ (this study, plain diamonds). PAR ($\mu\text{mol m}^{-2} \text{s}^{-1}$) and
720 temperature $T \times 10$ ($^{\circ}\text{C}$) were recorded inside the enclosure.

721 **List of tables**

722

723 Table 1: BVOC emitted by *Q. pubescens* (Qp4) and *A. monspessulanum* (Am) branches, 1st
724 and 2nd of June respectively, measured with a PTR-MS.

725 Daily mean ($n=30$) and maximum (parenthesis) BVOC branch emission rates ER are in μgC
726 $\text{g}_{\text{DM}}^{-1} \text{h}^{-1}$. Values are expressed \pm their SD.

727 ^a Measurement information measured inside the enclosure chamber are daily averaged; PAR
728 is in $\mu\text{mol m}^{-2} \text{s}^{-1}$, temperature T in $^{\circ}\text{C}$, relative humidity RH in %, photosynthetic net
729 assimilation Pn in $\mu\text{molCO}_2 \text{m}^{-2} \text{s}^{-1}$ and stomatal conductance Gw in $\text{mmolH}_2\text{O m}^{-2} \text{s}^{-1}$.

730 ^b Percentage of speciated BVOC relative to total BVOC and to non-isoprene BVOC (brackets)

731 ^c Emission factors EF ($\mu\text{gC g}_{\text{DM}}^{-1} \text{h}^{-1}$) were the best fit slope of ER vs $C_L \times C_T$ as in Guenther et
732 al. (1993).

733 ^d Total monoterpenes emissions measured from the PTR-MS were derived from absolute
734 concentrations at m/z 137.

735

736 Table 2: Environmental and physiological parameters recorded during isoprene
737 measurements on seven sunlit (Qpi) and two shaded (Qpi_{shade}) *Q. pubescens* branches.

738 PAR ($\mu\text{mol m}^{-2} \text{s}^{-1}$), temperature T ($^{\circ}\text{C}$), relative humidity RH (%), photosynthetic net
739 assimilation Pn ($\mu\text{molCO}_2 \text{m}^{-2} \text{s}^{-1}$) and stomatal conductance Gw ($\text{mmolH}_2\text{O m}^{-2} \text{s}^{-1}$) were
740 recorded inside the enclosure and averaged over 2:00-22:00. Daily emission rates ERd (μgC
741 $\text{g}_{\text{DM}}^{-1} \text{h}^{-1}$) were averaged over the n isoprene measurements of the sampled branch; values in
742 brackets are minimum-maximum.

743 Assimilated carbon emitted as isoprene C_{iso} (%) is given \pm their SD.

744 For every branch, isoprene emission rates ER_{br} and emission factor Is (as in Guenther et al.
745 1993) \pm their SD are given in $\mu\text{gC g}_{\text{DM}}^{-1} \text{h}^{-1}$ and $\text{ngC m}^{-2} \text{h}^{-1}$ (parenthesis)

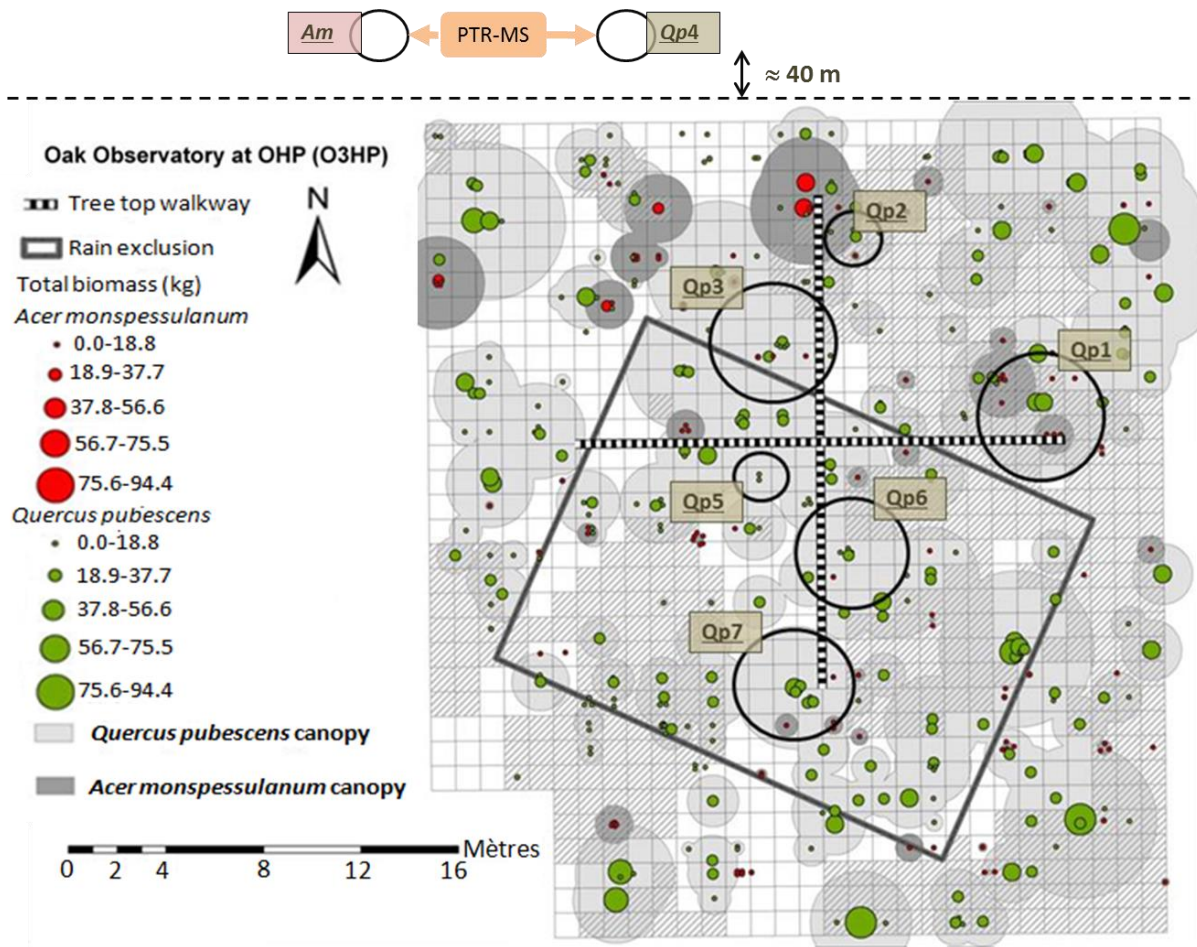
746

747 Table 3: Results of the comparison between calculated vs measured *Q. pubescens* isoprene
748 emission rates using, both, the G93 and MEGAN algorithm and an emission factor Is of (^a) 53
749 $\mu\text{gC g}_{\text{DM}}^{-1} \text{h}^{-1}$ (as in Simpson et al., 1999), and (^b) of 72 and 138 $\mu\text{gC g}_{\text{DM}}^{-1} \text{h}^{-1}$ ($Qp1$ and $Qp4$
750 respectively, this study). The $ax+b$ best fit equations are given, together with the
751 determination coefficient (R^2) and the root mean square error (RMSE).

752

753 Fig. 1

754

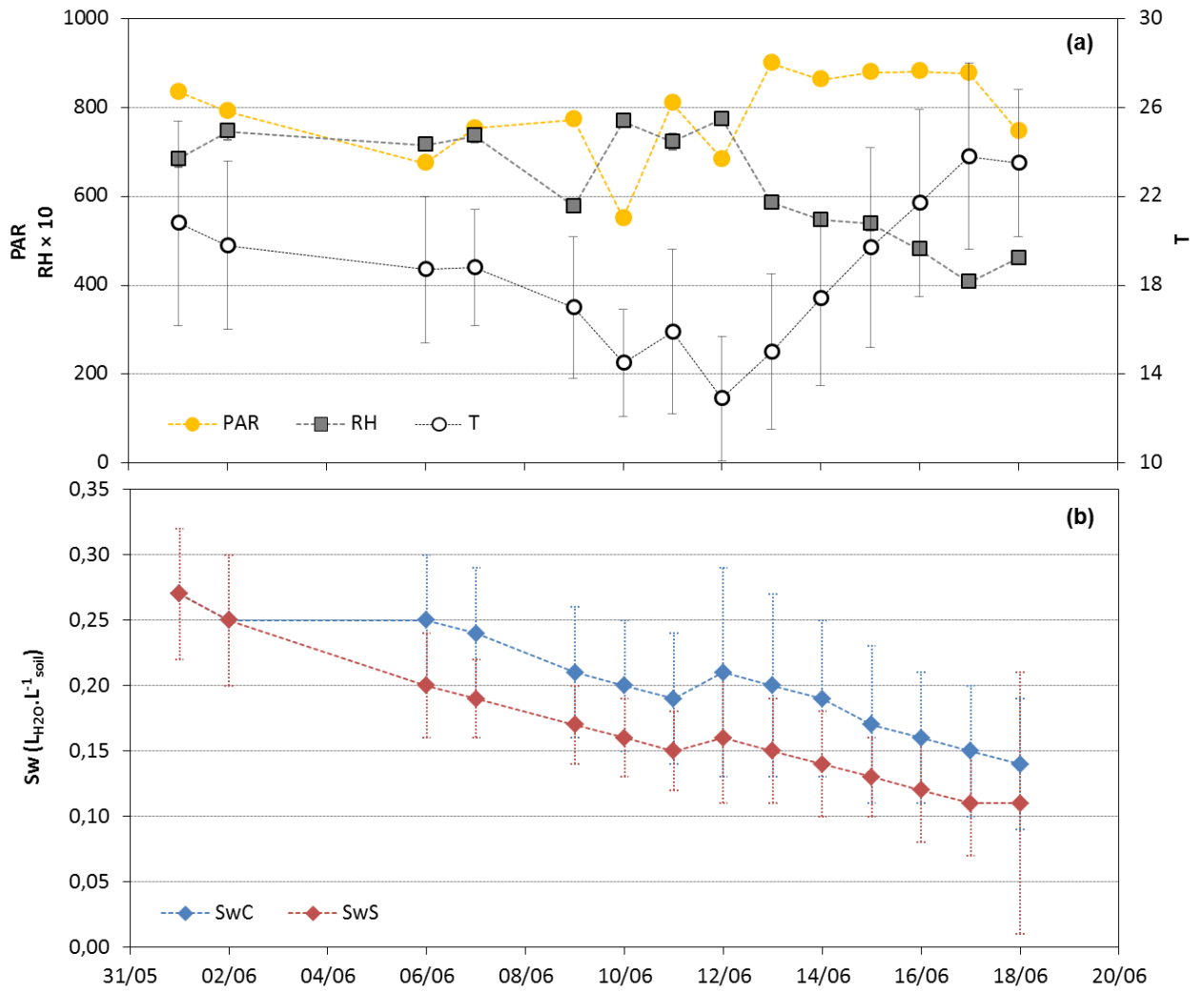


755

756

757 Fig. 2

758

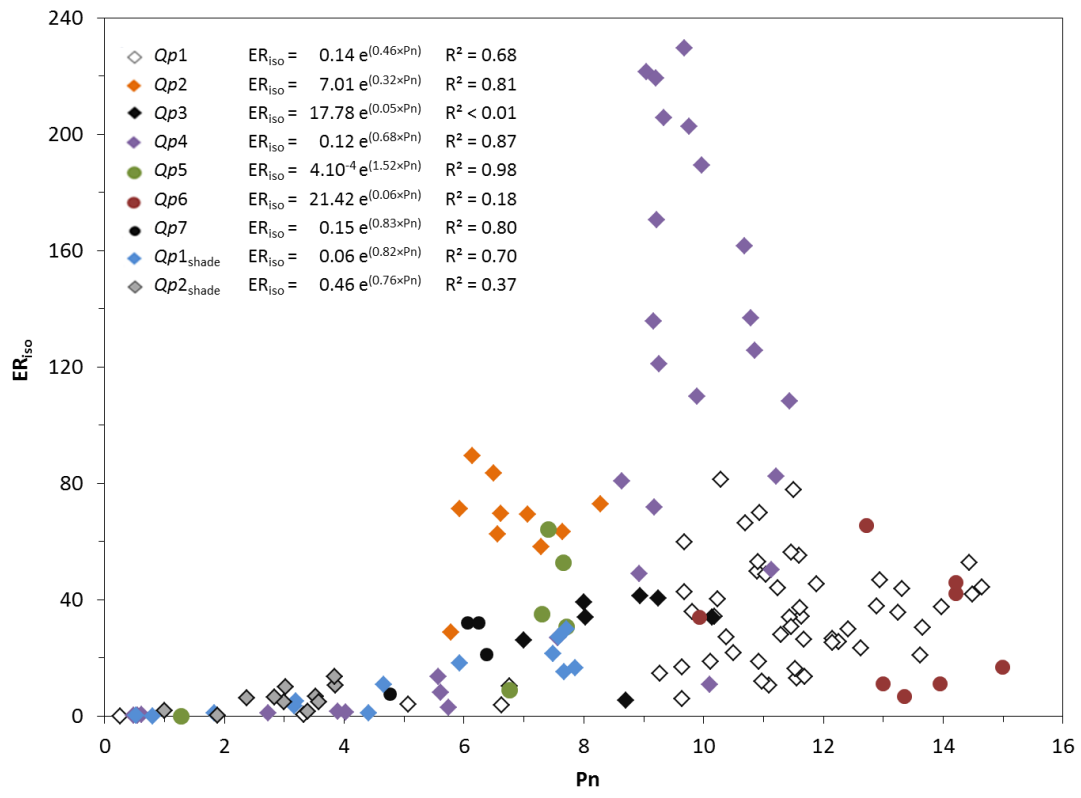


759

760

761 **Fig. 3**

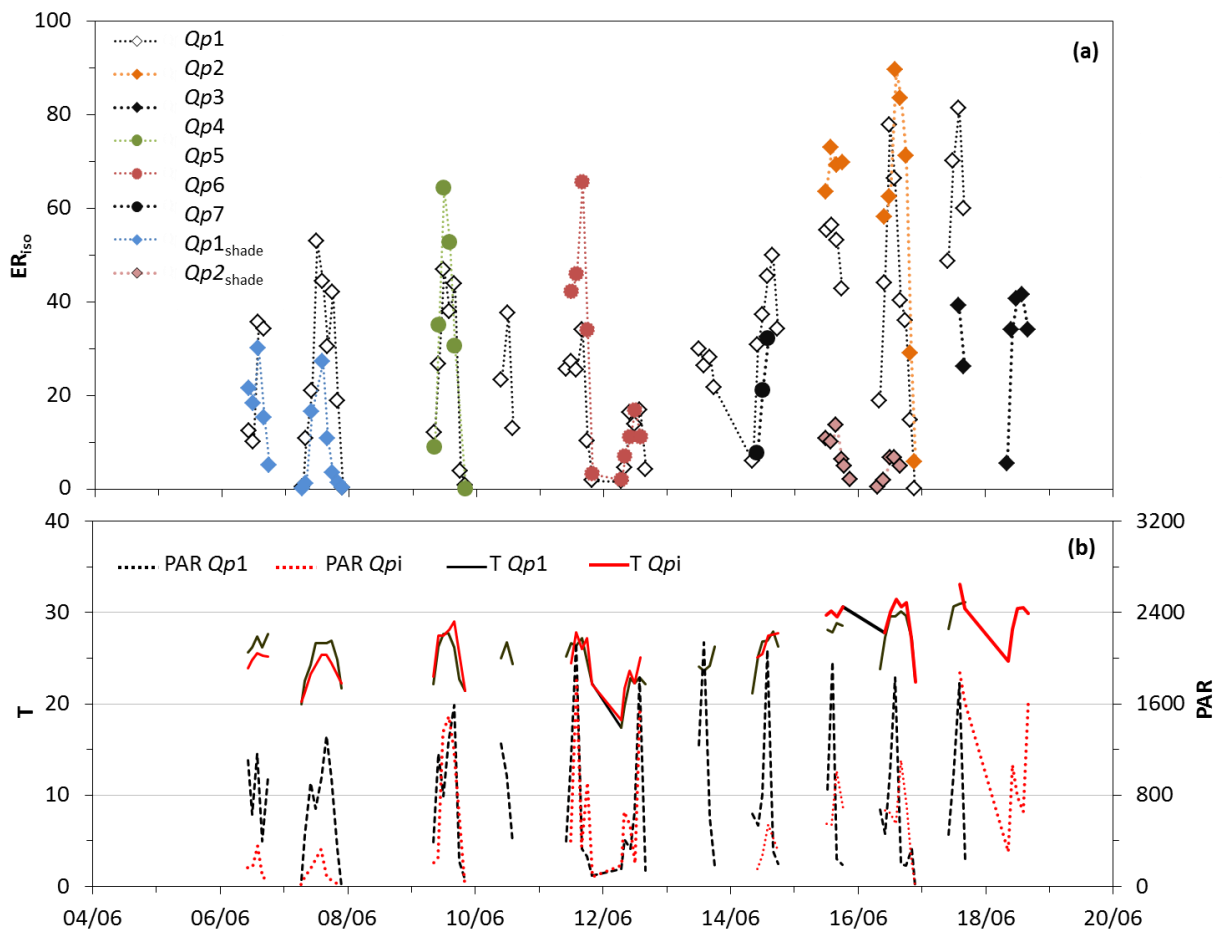
762



763

764 Fig. 4a and 4b

765



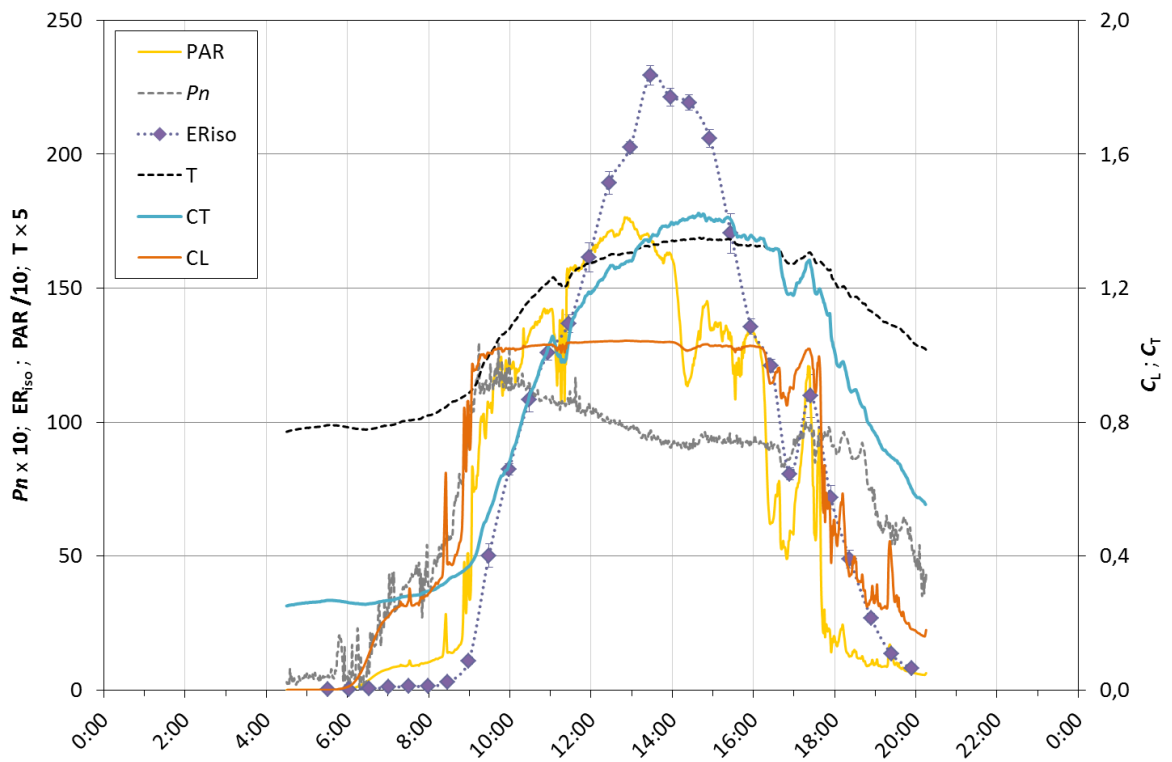
766

767

768

769 Fig. 5

770



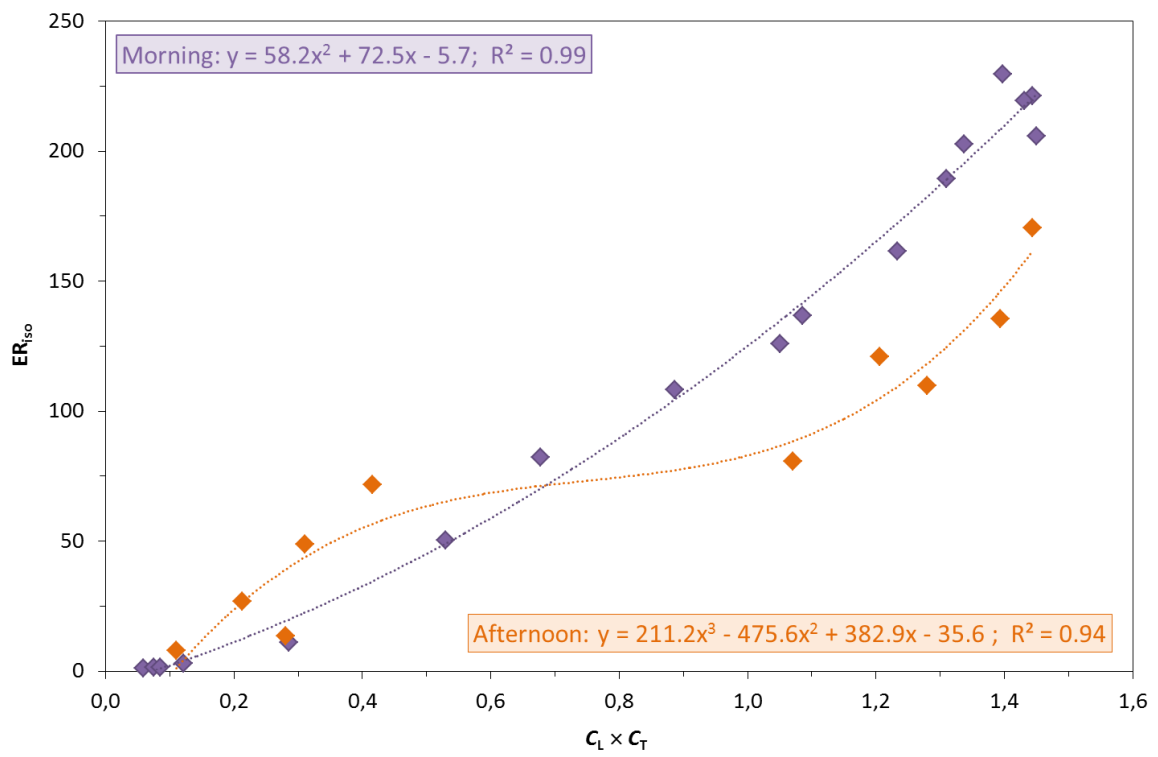
771

772

773

774 **Fig. 6**

775

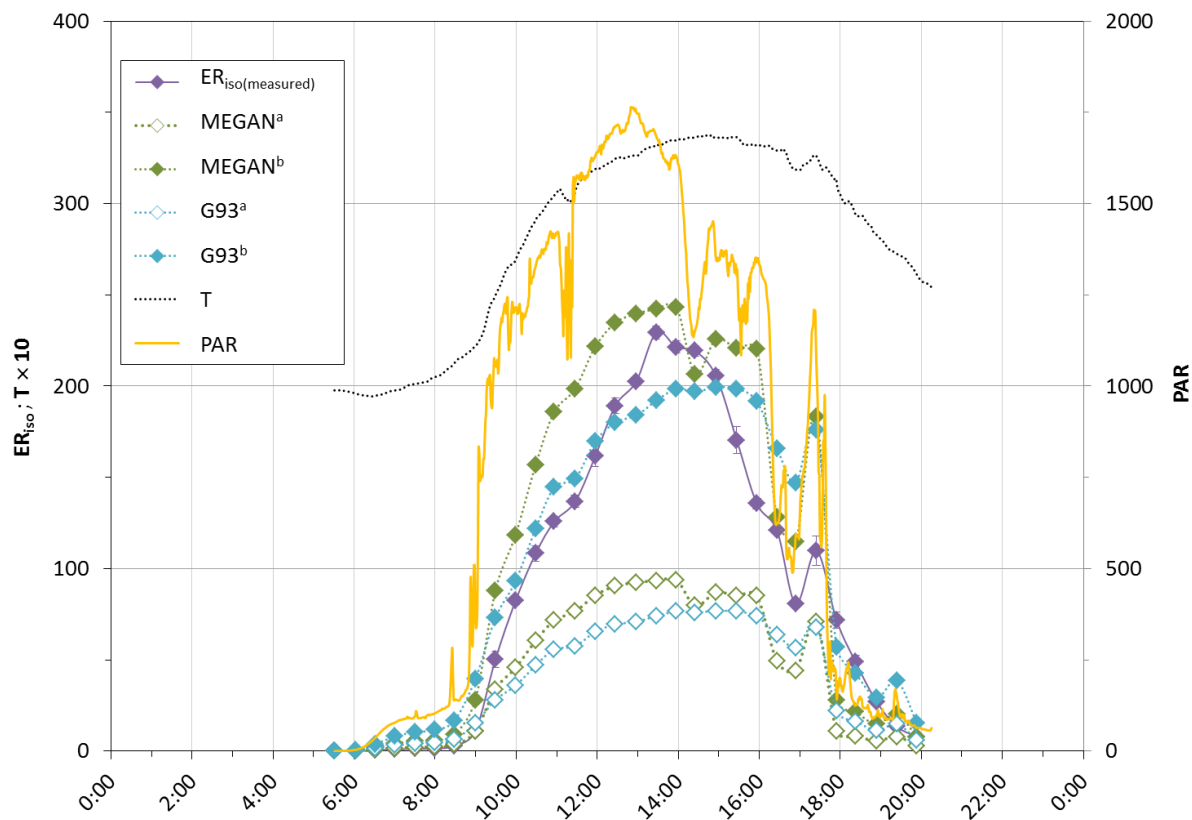


776

777

778 Fig. 7

779



780

781

782 **Table 1**

783

784

785

Compound	<i>Qp4</i>					<i>Am</i>				
	(PAR=851.7; T=28.7±4.9; RH=68.7±10.3; Pn=8.3±2.8; Gw=189.6±157.6) ^a					(PAR=460.9; T=26.6±4.4; RH=75.2±18.7; Pn=2.3±1,3; Gw=85.3±45.9) ^a				
	<i>ER</i>		Relative composition ^b		EF ^c	<i>ER</i>		Relative composition ^b		EF ^c
Methanol	0.49±0.10	(0.98)	0.5	{41.5}	0.50±0.04	0.23±0.08	(0.57)	26.7	{43.4}	0.39±0.04
Acetaldehyde	0.09±0.03	(0.30)	0.1	{7.6}	0.12±0.01	0.13±0.06	(0.38)	15.1	{24.5}	0.28±0.03
Acetone	0.20±0.06	(0.46)	0.2	{16.9}	0.27±0.02	0.14±0.04	(0.32)	16.3	{26.4}	0.24±0.02
Isoprene	98±31	(229)	98.8	-	138±10	0.33±0.09	(0.73)	38.4	-	0.47±0.04
MVK+MACR	0.10±0.03	(0.26)	0.1	{8.5}	0.15±0.01	0.01±0.005	(0.04)	1.2	{1.9}	0.030±0.002
Monoterpenes ^d	0.30±0.10	(0.77)	0.3	{25.4}	0.44±0.03	0.02±0.01	(0.07)	2.3	{3.8}	0.050±0.003

786

787

<i>Quercus pubescens</i> tree	<i>n</i>	Measurement information						ER _d	C _{iso}	ER _{br}	<i>I_S</i>		
		Date	PAR	T	RH	<i>P_n</i>	<i>G_w</i>						
Control plot	Qp4	28	1-Jun	851.7	28.7±4.9	68.7±10.3	8.3±2.8	189.6±157.6	98 {0.4-229}	2.7±2.2	98±31 (11.1±3.5)	138±10 (15.6±1.1)	
		4	6-Jun	851.7	26.6±0.9	66.2±4.5	12.4±1.1	263.7±31.0	23 {9.8-35}	0.8±0.1			
		9	7-Jun	625.9	24.5±2.5	70.8±5.3	11.6±5.0	228.9±137.4	24 {0.16-52}	0.6±0.3			
		7	9-Jun	780.5	24.9±2.7	64.4±6.7	10.3±3.8	191±99.9	24 {0.5-47}	0.6±0.4			
		3	10-Jun	868.3	25.4±1.2	61.1±6.0	12.7±1.2	155±27.4	24 {13-37}	0.5±0.2			
		6	11-Jun	725	25.4±1.8	58.6±3.2	10.6±2.3	154.5±47.2	21 {1.7-34}	0.6±0.2			
		Qp1	6	12-Jun	585.1	21.2±2.2	70.4±6.3	9.5±3.1	114.8±24.6	9.4 {1.4-17}	0.4±0.1	30±5 (3.7±0.6)	72±3 (8.8±0.3)
		4	13-Jun	1040.8	24.5±1.2	-	11.4±0.8	-	26 {22-30}	0.6±0.1			
		6	14-Jun	758	25.7±2.4	58.0±4.6	10.9±0.9	157.5±62.4	34 {5.8 -50}	0.9±0.4			
		4	15-Jun	810.9	28.4±0.4	56.0±4.4	10.9±0.9	268.1±75.1	52 {43-56}	1.3±0.1			
		8	16-Jun	584.7	27.4±2.9	55.1±6.0	9.1±3.6	177.7±86.2	37 {<d.l.-78}	1.0±0.6			
		4	17-Jun	858.1	30.3±1.4	50.9±4.3	10.4±0.6	243.2±48.4	65 {49-81}	1.8±0.4			
		Qp1 _{shade}	5	6-Jun	166.7	24.9±0.6	84.3±5.1	6.4±1.9	102.7±16.6	13 {3.5-21}	0.5±0.2	12±6 (1.0±0.6)	77±2 (6.7±0.2)
		8	7-Jun	92.1	23.1±1.9	80.1±10.1	3.8±2.8	54.0±62.6	5.3 {<d.l.-19}	0.3±0.2			
		Qp2	4	15-Jun	693.8	30.0±0.5	57.5±6.6	7.4±0.7	92.8±25.8	69 {63 -72}	2.7±0.3	61±16 (7.5±1.2)	74±4 (9.1±0.5)
	7	16-Jun	559.9	28.7±3.2	65.0±7.0	5.4±2.5	106.7±44.4	57 {5.6 -90}	2.9±1.0				
	Qp2 _{shade}	6	15-Jun	60,9	24.3±1.6	54.3±4.2	2.8±1.1	11.5±9.6	7.8 {1.9-14}	0.3±0.2	6.1±4.1 (0.5±0.4)	59±12 (5.1±0.1)	
	5	16-Jun	29,5	24.1±3.3	55.5±15.9	3.0±0.7	11.9±10.4	4.0 {0.3-6.6}	0.5±0.2				
	Qp3	2	17-Jun	1742.5	31.8±1.8	49.3±8.8	7.5±0.7	133.7±8.3	33 {26-39}	1.2±0.2	32±12 (3.9±1.1)	31±8 (3.8±1.0)	
	5	18-Jun	885.6	28.7±2.4	61.4±10.9	9.0±0.8	140.2±26.3	31 {5.2 -41}	1.0±0.5				

Rain exclusion plot	Qp5	6	9-Jun	757.6	26.1±3.1	65.5±8.1	6.3±2.5	68.8±26.4	31.9 {<d.l.-64}	1.2±0.9	31.9±25.8	(3.9±3.2)	58±17	(7.2±2.1)
	Qp6	5	11-Jun	708.6	25.5±2.3	60.7±9.2	12.8±2.0	130.1±46.8	38.1 {3.2-66}	1.2±0.9	23.8±15.5	(2.9±1.9)	54±13	(6.7±1.6)
		5	12-Jun	633.1	22.2±2.6	63.6±10.4	13.8±0.9	75.8±46.9	9.5 {1.8-17}	0.3±0.1				
	Qp7	4	14-Jun	318.2	26.4±1.3	65.8±5.1	5.9±0.7	62.5±26.7	23.1 {7.4-32}	1.1±0.5	23.2±18.5	(2.9±2.3)	62±8	(7.6±0.9)

790

791

792 **Table 3**

793

794

Tree		Is^a			Is^b		
		$ax + b$	R^2	RMSE	$ax + b$	R^2	RMSE
<i>Qp4</i>	G93	$0.35x + 6.96$	0.91	73.67	$0.92x + 18.05$	0.91	26.59
	MEGAN	$0.45x + 2.66$	0.92	65.89	$1.16x + 6.90$	0.92	36.69
<i>Qp1</i>	G93	$0.54x + 10.08$	0.74	11.88	$0.73x + 13.61$	0.74	11.61
	MEGAN	$0.23x + 9.00$	0.15	23.53	$0.32x + 12.14$	0.15	21.88

795

796

797 **Appendix**

798 **Supplementary materials: emission factor I_s calculation**

799

800 The empirical relationship used to describe changes in isoprene emission rates I ($\mu\text{gC g}_{\text{DM}}^{-1} \text{h}^{-1}$)
801 vs light and temperature was as in Guenther et al. (1993):

802

803
$$I = I_s \times C_T \times C_L \quad (\text{A1})$$

804

805 where

806 I_s is the isoprene emission factor standardised at $T = 30 \text{ }^\circ\text{C}$ and $\text{PAR} = 1000 \mu\text{mol m}^{-2} \text{s}^{-1}$ (μgC
807 $\text{g}_{\text{DM}}^{-1} \text{h}^{-1}$), and C_L and C_T are, respectively, light and temperature coefficient defined by

808
$$C_L = \frac{\alpha C_{L1} L}{\sqrt{1 + \alpha^2 L^2}} \quad (\text{A2})$$

809 and

810
$$C_T = \frac{e^{\frac{C_{T1}(T-T_s)}{RTTs}}}{1 + e^{\frac{C_{T2}(T-T_M)}{RTTs}}} \quad (\text{A3})$$

811 where $\alpha=0.0027 \text{ m}^2 \text{ s } \mu\text{mol}^{-1}$, $C_{L1}=1.066$ units, $C_{T1}=95000 \text{ J mol}^{-1}$, $C_{T2}=230000 \text{ J mol}^{-1}$, $T_M = 314$
812 K are empirically derived constants, L is the Photosynthetically Active Radiation (PAR) flux
813 ($\mu\text{mol}(\text{photon}) \text{ m}^{-2} \text{ s}^{-1}$), T is the predicted temperature (K), and T_s is the leaf temperature at
814 standard condition (303 K); at standard conditions of $1000 \mu\text{mol}(\text{photon}) \text{ m}^{-2} \text{ s}^{-1}$ PAR and 303
815 K, $C_T \times C_L=1$.

816 **References**

- 817 Atkinson, R.: Atmospheric chemistry of VOCs and NO_x, *Atmos. Environ.*, 34, 2063–2101,
818 doi:10.1016/S1352-2310(99)00460-4, 2000.
- 819 Von Caemmerer, S. and Farquhar, G. D.: Some relationships between the biochemistry of
820 photosynthesis and the gas exchange rates of leaves., *Planta*, 153, 376–387, 1981.
- 821 Chen, F. and Dudhia, J.: Coupling an advanced land surface-hydrology model with the Penn
822 State-NCAR MM5 modeling system. Part I: Model implementation and sensitivity, *Mon.*
823 *Weather Rev.*, 129(4), 569–585, 2001.
- 824 Ciccioli, P., Brancaleoni, E., Frattoni, M., Di Palo, V., Valentini, R., Tirone, G., Seufert, G.,
825 Bertin, N., Hansen, U., Csiky, O., Lenz, R. and Sharma, M.: Emission of reactive terpene
826 compounds from orange orchards and their removal by within-canopy processes, *J.*
827 *Geophys. Res.-Atmos.*, 104, 8077–8094, 1999.
- 828 Claeys, M., Graham, B., Vas, G., Wang, W., Vermeylen, R., Pashynska, V., Cafmeyer, J.,
829 Guyon, P., Andreae, M. O., Artaxo, P. and Maenhaut, W.: Formation of secondary organic
830 aerosols through photooxidation of isoprene, *Science*, 303, 1173–1176,
831 doi:10.1126/science.1092805, 2004.
- 832 Curci, G., Beekmann, M., Vautard, R., Smiatek, G., Steinbrecher, R., Theloke, J. and Friedrich,
833 R.: Modelling study of the impact of isoprene and terpene biogenic emissions on European
834 ozone levels, *J. Atmos. Env.*, 43, 1444–1455, doi:10.1016, 2009.
- 835 Damesin, C. and Rambal, S.: Field study of leaf photosynthetic performance by a
836 Mediterranean deciduous oak tree (*Quercus pubescens*) during a severe summer drought,
837 *New Phytol.*, 131, 159–167, doi:10.1111/j.1469-8137.1995.tb05717.x, 1995.
- 838 Fall R., Karl T., Hansel A., Jordan A. and Lindinger, W.: Volatile organic compounds emitted
839 after leaf wounding: On-line analysis by proton-transfer-reaction mass spectrometry. *J.*
840 *Geophys. Res.-Atmos.*, 104, 15963-15974, doi:10.1029/1999JD900144, 1999.
- 841 Fortunati, A., Barta, C., Brillì, F., Centritto, M., Zimmer, I., Schnitzler, J. P. and Loreto, F.:
842 Isoprene emission is not temperature-dependent during and after severe drought-stress: a
843 physiological and biochemical analysis, *Plant J.*, 55, 687–697, doi:10.1111/j.1365-
844 313X.2008.03538.x, 2008.
- 845 Funk, J. L., Mak, J. E. and Lerdau, M. T.: Stress-induced changes in carbon sources for
846 isoprene production in *Populus deltoides*, *Plant Cell Environ.*, 27, 747–755,
847 doi:10.1111/j.1365-3040.2004.01177.x, 2004.
- 848 Galbally I.E. and Kirstine W.: The production of methanol by flowering plants and the global
849 cycle of methanol. *J. Atmos. Chem.*, 43, 195-229, 2002.
- 850 Guenther, A. B., Monson, R. K. and Fall, R.: Isoprene and monoterpene emission rate
851 variability- Observation with *Eucalyptus* and emission rate algorithm development, *J.*
852 *Geophys. Res.-Atmos.*, 96, 10799–10808, doi:10.1029/91JD00960, 1991.

853 Guenther, A. B., Zimmerman, P. R., Harley, P. C., Monson, R. K. and Fall, R.: Isoprene and
854 Monoterpene Emission Rate Variability - Model Evaluations and Sensitivity Analyses, J.
855 Geophys. Res.-Atmos., 98, 12609–12617, doi:10.1029/93JD00527, 1993.

856 Guenther, A.B., Zimmerman, P. and Wildermuth, M.: Natural volatile organic compound
857 emission rate estimates for US woodland landscapes, Atmos. Environ., 28(6), 1197–1210,
858 doi:10.1016/1352-2310(94)90297-6, 1994.

859 Guenther, A.B, Hewitt, C.N., Erickson, D., Fall, R., Geron, C., Graedel, T., Harley, P., Klinger, L.,
860 Lerdau, M., Mckay, W.A., Pierce, T., Scholes, B., Steinbrecher, R., Tallamraju, R., Taylor, J.,
861 and Zimmerman, P.: A Global-Model of Natural Volatile Organic-Compound Emissions. J.
862 Geophys. Res.-Atmos, 100, 8873–8892, doi:10.1029/94JD02950, 1995.

863 Guenther, A., Karl, T., Harley, P., Wiedinmyer, C., Palmer, P. I. and Geron, C.: Estimates of
864 global terrestrial isoprene emissions using MEGAN (Model of Emissions of Gases and
865 Aerosols from Nature), Atmos. Chem. Phys., 6, 3181–3210, 2006.

866 Harley, P., Archer, S. and Guenther, A.: Effects of growth irradiance, nitrogen nutrition and
867 watering regime on photosynthesis, leaf conductance and isoprene emission in leaves of
868 Post Oak, *Quercus stellata*, Ecol. Soc. America, 75(2), 87-88, 1994.

869 Hayward, S., Tani, A., Owen, S. M. and Hewitt, C. N.: Online analysis of volatile organic
870 compound emissions from Sitka spruce (*Picea sitchensis*), Tree Physiol., 24(7), 721–728, doi:
871 10.1093/treephys/24.7.721, 2004.

872 Jardine, K. J., Monson, R. K., Abrell, L., Saleska, S. R., Arneth, A., Jardine, A., Ishida, F. Y.,
873 Serrano, A. M. Y., Artaxo, P. and Karl, T.: Within-plant isoprene oxidation confirmed by direct
874 emissions of oxidation products methyl vinyl ketone and methacrolein, Glob. Change Biol.,
875 18(3), 973–984, doi: 10.1111/j.1365-2486.2011.02610.x, 2012.

876 Kalogridis, C., Gros, V., Sarda-Esteve, R., Langford, B., Loubet, B., Bonsang, B., Bonnaire, N.,
877 Nemitz, E., Genard, A.-C., Boissard, C., Fernandez, C., Ormeño, E., Baisnée, D., Reiter, I. and
878 Lathièrre, J.: Concentrations and fluxes of isoprene and oxygenated VOCs at a French
879 Mediterranean oak forest, Atmos. Chem. Phys., 14, 10085-10102, doi:10.5194/acpd-14-
880 10085-2014, 2014.

881 Keenan, T., Niinemets, Ü., Sabate, S., Gracia, C. and Penuelas, J.: Process based inventory of
882 isoprenoid emissions from European forests: model comparisons, current knowledge and
883 uncertainties, Atmos. Chem. Phys., 9, 4053–4076, doi:10.5194/acp-9-4053-2009, 2009.

884 Kesselmeier, J., Bode, K., Schafer, L., Schebeske, G., Wolf, A., Brancaleoni, E., Cecinato, A.,
885 Ciccioli, P., Frattoni, M., Dutaur, L., Fugit, J. L., Simon, V. and Torres, L.: Simultaneous field
886 measurements of terpene and isoprene emissions from two dominant Mediterranean oak
887 species in relation to a north American species, Atmos. Environ., 32, 1947–1953,
888 doi:10.1016/S1352-2310(97)00500-1, 1998.

889 Kesselmeier, J. and Staudt, M.: Biogenic Volatile Organic Compounds (VOC): an overview on
890 emission, physiology and ecology, J. Atmos. Chem., 33, 23–88, 1999.

- 891 Loreto, F. and Sharkey, T.: On the relationship between isoprene emission and
892 photosynthetic metabolites under different environmental conditions. *Planta*, 189, 420-424,
893 doi:10.1007/BF00194440, 1993.
- 894 Monson, R. K. and Fall, R.: Isoprene Emission from Aspen Leaves : Influence of Environment
895 and Relation to Photosynthesis and Photorespiration, *Plant Physiol.*, 90, 267–274,
896 doi:<http://dx.doi.org/10.1104/pp.90.1.267>, 1989.
- 897 Niinemets, Ü. and Reichstein, M.: Controls on the emission of plant volatiles through
898 stomata: differential sensitivity of emission rates to stomatal closure explained. *J. Geophys.*
899 *Res.*, 108: doi: 10.1029/2002JD002620, 2003.
- 900 Niinemets, Ü., Arneth, A., Kuhn, U., Monson, R. K., Penuelas, J. and Staudt, M.: The emission
901 factor of volatile isoprenoids: stress, acclimation, and developmental responses,
902 *Biogeosciences*, 7, 2203–2223, doi:10.5194/bg-7-2203-2010, 2010a.
- 903 Niinemets, Ü., Monson, R. K., Arneth, A., Ciccioli, P., Kesselmeier, J., Kuhn, U., Noe, S. M.,
904 Penuelas, J. and Staudt, M.: The leaf-level emission factor of volatile isoprenoids: caveats,
905 model algorithms, response shapes and scaling, *Biogeosciences*, 7(6), 1809–1832,
906 doi:10.5194/bg-7-1809-2010, 2010b.
- 907 Owen, S. M., Boissard, C., Hagenlocher, B. and Hewitt, C. N.: Field studies of isoprene
908 emissions from vegetation in the Northwest Mediterranean region, *J. Geophys. Res.*, 103,
909 25499–25511, doi:10.1029/98JD01817, 1998.
- 910 Pollmann, J., Ortega, J. and Helmig, D.: Analysis of atmospheric sesquiterpenes: Sampling
911 losses and mitigation of ozone interferences, *Environ. Sci. Technol.*, 39(24), 9620–9629,
912 doi:10.1021/es050440w, 2005.
- 913 Seco, R., Penuelas, J. and Filella, I.: Short-chain oxygenated VOCs: Emission and uptake by
914 plants and atmospheric sources, sinks, and concentrations, *Atmos. Environ.*, 41(12), 2477–
915 2499, doi:10.1016/j.atmosenv.2006.11.029, 2007.
- 916 Simon, V., Dumergues, L., Bouchou, P., Torres, L. and Lopez, A.: Isoprene emission rates and
917 fluxes measured above a Mediterranean oak (*Quercus pubescens*) forest, *Atmos. Res.*, 74,
918 49–63, doi:10.1016/j.atmosres.2004.04.005, 2005.
- 919 Simpson, D., Winiwarter, W., Börjesson, G., Cinderby, S., Ferreiro, A., Guenther, A., Hewitt, C.
920 N., Janson, R., Khalil, M. A. K. and Owen, S.: Inventorying emissions from nature in Europe, *J.*
921 *Geophys. Res. Atmos.*, 104(D7), 8113–8152, doi: 10.1029/98JD02747, 1999.
- 922 Steinbrecher, R., Contran, N., Gugerli, F., Schnitzler, J.-P., Zimmer, I., Menard, T. and
923 Günthardt-Goerg, M. S.: Inter-and intra-specific variability in isoprene production and
924 photosynthesis of Central European oak species, *Plant Biol.*, 15(s1), 148–156,
925 doi:10.1111/j.1438-8677.2012.00688.x, 2013.
- 926 Steiner A. and Goldstein A.: *Volatile Organic Compounds in the Atmosphere*, Koppmann R.,
927 Blackwell publishing, United Kingdom, 2007.

928 Tani, A., Tozaki, D., Okumura, M., Nozoe, S. and Hirano, T.: Effect of drought stress on
929 isoprene emission from two major *Quercus* species native to East Asia, J. Atmos. Environ.,
930 45, 6261–6266, doi:10.1016/j.atmosenv.2011.08.003, 2011.